NeuroImage: Clinical 36 (2022) 103244

Contents lists available at ScienceDirect

NeuroImage: Clinical

journal homepage: www.elsevier.com/locate/ynicl

Advanced spinal cord MRI in multiple sclerosis: Current techniques and future directions

Anna J.E. Combes [a,b,*], Margareta A. Clarke [a], Kristin P. O'Grady [a,b,c], Kurt G. Schilling [a,b], Seth A. Smith [a,b,c]

[a] Vanderbilt University Institute of Imaging Science, Vanderbilt University Medical Center, 1161 21st Avenue South, Medical Center North, AA-1105, Nashville, TN 37232-2310, United States

[b] Department of Radiology and Radiological Sciences, Vanderbilt University Medical Center, Medical Center North, 1161 21st Ave. South, Nashville, TN 37232, United States

[c] Department of Biomedical Engineering, Vanderbilt University, 2301 Vanderbilt Place, PMB 351826, Nashville, TN 37235-1826, United States

ARTICLE INFO

Keywords:
Spinal cord
Multiple sclerosis
advanced MRI
quantitative MRI
functional MRI

ABSTRACT

Spinal cord magnetic resonance imaging (MRI) has a central role in multiple sclerosis (MS) clinical practice for diagnosis and disease monitoring. Advanced MRI sequences capable of visualizing and quantifying tissue macro- and microstructure and reflecting different pathological disease processes have been used in MS research; however, the spinal cord remains under-explored, partly due to technical obstacles inherent to imaging this structure. We propose that the study of the spinal cord merits equal ambition in overcoming technical challenges, and that there is much information to be exploited to make valuable contributions to our understanding of MS.

We present a narrative review on the latest progress in advanced spinal cord MRI in MS, covering in the first part structural, functional, metabolic and vascular imaging methods. We focus on recent studies of MS and those making significant technical steps, noting the challenges that remain to be addressed and what stands to be gained from such advances. Throughout we also refer to other works that presend more in-depth review on specific themes. In the second part, we present several topics that, in our view, hold particular potential. The need for better imaging of gray matter is discussed. We stress the importance of developing imaging beyond the cervical spinal cord, and explore the use of ultra-high field MRI. Finally, some recommendations are given for future research, from study design to newer developments in analysis, and the need for harmonization of sequences and methods within the field.

This review is aimed at researchers and clinicians with an interest in gaining an overview of the current state of advanced MRI research in this field and what is primed to be the future of spinal cord imaging in MS research.

1. Introduction

Imaging of the spinal cord (SC) with magnetic resonance imaging (MRI) plays a central role in the diagnosis and clinical management of multiple sclerosis (MS). Assessment of SC pathology has value in predicting accrual of disability and conversion to a progressive course (Bischof et al., 2022; Ruggieri et al., 2021); recently introduced concepts like the topographical model of MS (Krieger et al., 2016) and the idea of SC 'reserve' (Sastre-Garriga et al., 2022b) also stress its importance and prognostic value. As technical advances are made, SC imaging has the potential to provide markers able to quantify axonal and myelin damage, protection and repair; to improve our understanding of MS pathology beyond radiological observations; and ultimately to provide outcome measures for clinical trials and to monitor patients over time.

In this paper, we focus on research MRI applications in the SC in MS at high field strength. Two recent reviews (Chen et al., 2020; Moccia et al., 2019) have to be mentioned that summarize advances and perspectives in SC imaging for MS; we build upon these and others by offering a perspective on the most promising topics in current research.

In the first part, we go over current techniques used for assessing SC tissue structure and microstructure. Discussed below are recent advancements in diffusion MRI, myelin water imaging, and saturation transfer-based methods. We then go over the methods for assessing function and metabolism, including functional MRI (fMRI),

* Corresponding author at: 1161 21st Ave S, MCN AA1105, Nashville, TN 37232, USA.
E-mail address: anna.combes@vumc.org (A.J.E. Combes).

https://doi.org/10.1016/j.nicl.2022.103244
Received 30 April 2022; Received in revised form 2 September 2022; Accepted 19 October 2022
Available online 21 October 2022
2213-1582/© 2022 The Authors. Published by Elsevier Inc. This is an open access article under the CC BY-NC-ND license (http://creativecommons.org/licenses/by-nc-nd/4.0/).

spectroscopy and susceptibility-based imaging. While issues of validation and reproducibility, which are crucial to clinical translation, are discussed throughout, we refer to work by Granziera et al. (2021) for a more comprehensive reflection on the clinical maturity of these methods.

In the second part, we discuss topics deemed relevant to the future of the field, highlighting the need for improved imaging of gray matter (GM) pathology; imaging beyond the cervical cord, and the value of concurrent brain-SC imaging; and going over necessary methodological advancements, including the use of ultra-high field (UHF) and considerations on study design and analysis methods.

2. Advanced imaging methods

2.1. Macro- and microstructural imaging

2.1.1. Diffusion MRI

Diffusion MRI (dMRI) harnesses the diffusion of water molecules, restricted and influenced by interactions with tissue components including macromolecules and membranes, to generate image contrast. In the SC, this offers the potential to detect and characterize specific tissue and cell types and measure changes associated with pathology. The commonly used diffusion tensor imaging (DTI) results in quantitative measures describing the magnitude of diffusion both perpendicular and parallel to the cord (radial and axial diffusivities) as well as measures of the coherence of the diffusion process (fractional anisotropy). DTI measures have shown a strong correlation with EDSS scores, providing solid evidence that microstructural changes contribute to disability (Kearney et al., 2015). For example, decreased anisotropy and increased radial diffusivity are observed in the MS cord compared to controls (Kearney et al., 2015; Klawiter et al., 2011; Toosy et al., 2014). However, while DTI measures are highly sensitive, they are not specific to any individual changes in tissue microstructure (Jones and Cercignani, 2010; Wheeler-Kingshott and Cercignani, 2009).

Here, biophysical models (or multi-compartment models) offer a solution in attempting to explicitly characterize the geometry, size, and diffusion properties of individual tissue compartments, resulting in potentially more meaningful and specific parameters of the tissue microstructure (Jelescu et al., 2016, 2015; Novikov et al., 2019, 2018). For example, offering the ability to measure neurite orientations and dispersion, the intra- and extra- axonal volume fractions and diffusivities (Jelescu et al., 2015; Kaden et al., 2016; Palombo et al., 2020; Zhang et al., 2012), soma and dendritic cell sizes (Palombo et al., 2020), free water partial volume (Pasternak et al., 2009; Zhang et al., 2012), or even axon radii (Alexander et al., 2010; Assaf et al., 2008; Barazany et al., 2009; Fan et al., 2018; Veraart et al., 2020) thus allowing to provide more specific information about pathology, separating and quantifying edema, demyelination, or axonal loss. This is particularly important in light of the fact that current clinical protocols do not provide that pathological specificity. Despite this potential, multi-compartment models of diffusion have been rarely implemented in the cord (By et al., 2018b, 2017; Collorone et al., 2020; Grussu et al., 2020, 2019, 2017, 2015; Schilling et al., 2019b), and even less in MS pathology (By et al., 2017; Collorone et al., 2020; Grussu et al., 2017). Improvements and innovation in acquisition, pre-processing, and biophysical modelling are needed to make SC diffusion MRI a useful biomedical tool for MS.

Although a standard protocol was recently proposed and validated to serve as a starting point for clinicians and researchers studying the cord with dMRI (Cohen-Adad et al., 2021b), advances are needed to acquire high SNR data (particularly relevant for dMRI where the diffusion process already attenuates the MR signal), with resolution high enough to ensure intra-cord contrast while minimizing distortions. This may include optimized diffusion encoding (Jones et al., 1999; Landman et al., 2007), or patient-specific diffusion encoding schemes to take advantages of the orientation of the cord, reduced field-of-view or multi-shot acquisition schemes (Jeong et al., 2013; Karampinos et al., 2009; Wilm et al., 2007) to minimize distortions, or investigations of alternative readouts (e.g., turbo/fast spin echo, propeller), to get the most SNR out of images.

Advances are also expected in pre-processing. The excellent review by Tax et al. covers new and novel pre-processing strategies developed for diffusion MRI (Tax et al., 2022); here, future developments and improvements are anticipated using deep learning networks for tissue masking (Kleesiek et al., 2016), utilizing complex data (Cordero-Grande et al., 2019), data redundancy (Veraart et al., 2016), or machine learning (Fadnavis et al., 2020) for noise bias removal or denoising, advances in signal representation for motion and outlier detection (Christiaens et al., 2021; Tax et al., 2015), and deep learning for distortion corrections (Qiao and Shi, 2020; Schilling et al., 2019a, 2020). While most of these are developed and optimized for the brain, the Spinal Cord Toolbox (SCT; see 'Analysis tools' section) already offers motion correction, cord masking, and robust model fitting for dMRI. Moreover, denoising algorithms have shown feasibility in the cord using high-quality, multi-contrast datasets (Grussu et al., 2020) and on clinical quality low-direction diffusion datasets (Schilling et al., 2021). Nevertheless, advances are still needed to improve susceptibility distortion and motion correction (Snoussi et al., 2021), particularly at high b-values and with low SNR data.

While as described above, diffusion modelling has shown feasibility using SC data, little validation has been performed specifically in the cord, which may have different tissue microstructural characteristics than many fiber pathways in the brain – including larger or more heterogenous axon diameters, different GM constituents, and more extreme partial volume effects. Future works should investigate which biophysical models are appropriate for the cord; for example, it may be possible to sensitize sequences to the larger axon diameters, and models utilizing stick-components (i.e. zero radius axons) may be less appropriate. It will be critical to assess existing and new models for the cord, and the MS cord in particular, evaluating not only model fit, but also sensitivity and specificity to physiological changes in the tissue (Jelescu et al., 2020). Additionally, multi-dimensional or advanced diffusion encodings (Andersen et al., 2020; Lundell et al., 2019; Nery et al., 2019; Topgaard, 2017; Westin et al., 2016), which may enable robust model fitting or enhanced sensitivity to specific tissue features (different scales of anisotropy, size variances, orientational coherence) have been underexplored in the SC.

Reproducibility of dMRI of the SC has been thoroughly characterized for within sessions (i.e., scan-rescan), across sites, and across vendors. A study of a single subject scanned in 19 centers, and 260 subjects scanned at 42 centers enabled the production of normative values within and along the SC (Cohen-Adad et al., 2021a). Notably, while DTI measures show very little intra- and inter-site variability, there were significant differences across vendors, largely attributed to noise properties, coils, reconstruction, and different strategies for reducing field of view and motion correction (Cohen-Adad et al., 2021a, 2021b). Similarly, normative values have been provided for multi-compartment models, including NODDI and Spherical Mean Techniques (By et al., 2018b; Grussu et al., 2015; Schilling et al., 2019b), again showing high reproducibility, even with clinically feasible acquisitions (By et al., 2018b, 2016).

Lastly, diffusion MRI enables mapping the structural connections of the CNS through fiber tractography (Basser et al., 2000; Behrens et al., 2003; Catani et al., 2002). While this may seem rather uninteresting in the cord, typically resulting in a single large superior-inferiorly orientated bundle, improvements in acquisition, pre-processing, and modelling of the cord may facilitate enhanced structural connectomic investigations. Future work may also utilize tractography to study intra-segment connections, cluster or parcellate ascending or descending pathways of the cord, or integrate brain and cord structural connections (see 'Brain and cord imaging' section).

2.1.2. Myelin imaging

2.1.2.1. Myelin water imaging. Myelin water imaging (MWI) is a traditionally T_2 relaxation-based method for the quantification of myelin water fraction, a surrogate measure of myelin content. MWI was recently identified by MAGNIMS (Granziera et al., 2021), along with quantitative T_1 mapping and MTR, as among the most 'mature', and the furthest along towards clinical applicability and utility among several advanced SC imaging techniques. The advantages of MWI are the relatively high reproducibility and specificity for myelin. While brain MWI has already made several contributions to the understanding of structure vs function relationships in MS (see (Edwards et al., 2022) for a review), there remains room for applying the same designs in the SC. (Lee et al., 2020) point out several barriers to the further deployment of MWI, including the limited vendor availability of most advanced sequences, and the complexity of the post-processing. To help remedy this, improvements have been made recently in terms of rapid imaging, ease and speed of processing, specificity and stability of algorithm fitting methods, and availability of normative datasets. Ljungberg et al. (2017) implemented a 3D gradient and spin echo (GRASE) T_2 relaxation experiment covering 4 cm at the C2-C3 level in the inferior-posterior direction in a 8.5 min acquisition, which showed sensitivity to lesional damage in MS (Dvorak et al., 2019) and helped differentiate between relapsing and progressive subtypes (Lee et al., 2021). Liu et al. (2020b) optimized a fitting algorithm using a neural network as an alternative to the existing NNLS method for T_2 decay curve fitting, taking the processing time from 15 min to 4 s for single-subject GRASE data, further reducing hardware and computing demands and thus bringing it closer to large-scale feasibility. Liu et al. (2020a) employed z-score mapping to highlight abnormal areas of myelin water fraction (MWF) and geometric mean T_2 in the cervical SC (CSC) in three participants with relapsing-remitting MS (RRMS) compared to a control group, using the aforementioned GRASE sequence. One could envision further applications of this method for the visualization and quantification of damage assessed by MWI, provided that compatibility with data from different scanners/sequences, greater anatomical coverage, and inclusion of a control population with broader demographic characteristics could be achieved. Moreover, Dvorak et al. (2021) compared T_2-based MWI methods in controls and people with MS (pwMS; mcDESPOT vs GRASE), and discussed both with regards to sensitivity to MS-related demyelination in brain and CSC. Use of MWI in the SC in MS is supported by ongoing work on histological validation in both healthy and MS brain and cord tissue (see Laule and Moore, 2018 for a review), including making use of UHF (Laule et al., 2016; McDowell et al., 2022), as well as a substantial body of work on acquisition strategies, algorithm stability, and intra- and inter-site reproducibility (Alonso-Ortiz et al., 2015).

Somewhat akin to myelin water imaging, the Rapid Estimation of Myelin for Diagnostic Imaging (REMyDI), a variant of synthetic imaging based on fast, simultaneous measurement of T_1, T_2 and proton density, enables reconstruction of various image contrasts with different weightings, including 'myelin fraction' maps (Warntjes et al., 2016). Preliminary result have shown good repeatability and inter-site reproducibility, and sensitivity to MS myelin pathology *in* and *ex vivo* in the brain (Ouellette et al., 2020a); adaptation to the SC would represent another promising development in myelin quantification.

2.1.2.2. Magnetization transfer and quantitative MT. Magnetization Transfer (MT) MRI is one of several MRI methods that can provide sensitivity to myelin damage, loss and repair. MT imaging has been extensively explored in the brain and, to a lesser degree, in the SC, primarily due to the simplicity of the pulse sequence and relative ease of post-processing. The MT Ratio (MTR) has been shown to be sensitive to de- and re-myelination (Chen et al., 2008), yet uncertainty still remains about its specificity for myelin (Vavasour et al., 2011) and its reproducibility (van der Weijden et al., 2021), including in the SC specifically (Combès et al., 2019; Lévy et al., 2018). As such, it is not ideally positioned to be considered for large, multi-center trials due to its sensitivity to pulse sequence design, non-physiological indices, vendor differences, and field strength.

To that end, quantitative MT (qMT) has been designed to calculate physiological parameters such as the pool size ratio (PSR), the related metric macromolecular pool fraction (MPF), and MT exchange rate. QMT-derived indices have shown sensitivity to differences in myelin content between brain normal-appearing white matter (WM), de- and re-myelinated MS lesions in post-mortem brain tissue (Schmierer et al., 2007), and correlated strongly with myelin in a number of animal validation studies (Kisel et al., 2022); development and applications to study MS pathology in brain GM and WM have been numerous (York et al., 2022). However, qMT can in practice be quite slow. Whether performed by selective inversion recovery (SIR) or pulsed saturation (Smith et al., 2017), multiple images must be obtained and co-registered. In the SC, the number of acquisitions in combination with the demand for high resolution can lead to very long and prohibitive scan times. In addition, the fitting routines required to extract these parameters are computationally costly, all of which currently presents significant challenges against potential clinical adoption. Conversely, using the qMT formalism presented by Yarnykh et al. (Yarnykh, 2012), Smith et al. (2017) showed that B_1 and B_0-corrected single-point qMT can, indeed, be performed in the SC with improved scan time and sensitivity to MS pathology. As seen in Fig. 1, the PSR (and ΔPSR: the difference in PSR for a participant with MS compared to a control group average) is reduced throughout the SC, which may reflect the presence of demyelinating lesions. Other approaches for acquisition in the SC have been proposed: *EPI*-based with a reduced field-of-view, which showed adequate single-subject reproducibility and agreement of quantitative indices with previous work (Battiston et al., 2018), and another as part of a multi-parametric protocol with unified read-out (Grussu et al., 2020). Both currently await application to MS.

Looking forward, the two most pressing needs for SC qMT and their application to MS are as follows. First is scan efficiency: minimizing scan time while maintaining high-fidelity, high-confidence PSR calculations. The single-point method shows that it is possible to calculate the PSR in the SC of pwMS while correcting for non-physiological variables; however, it has not been studied in large trials or across vendors. More sophisticated approaches such as artificial intelligence (AI) or deep learning could be considered to improve the fitting of noisy data or to minimize the number of acquisitions necessary for high-fidelity PSR indices. Secondly, further understanding the sensitivity and specificity of MT in the SC to de- and re-myelination could have applications in clinical trials of MS.

2.1.2.3. Inhomogeneous magnetization transfer. As stated above, conventional MT imaging, including MTR and qMT, lacks specificity for myelin, since MT imaging reflects the communication between all macromolecular protons and water. An alternative approach, inhomogeneous MT (ihMT), has been developed and utilizes the differences in saturation transfer among three different saturation schemes: saturation at positive offset frequencies, saturation at negative offset frequencies, and dual frequency saturation (positive and negative) to improve specificity for myelin rich tissues. ihMT has shown higher GM:WM contrast, as well as sensitivity to MS lesions in the brain (Van Obberghen et al., 2018). The promise of increased specificity for myelin content and loss is enticing; however, ihMT also suffers from long acquisition times, sensitivity to B_1, and other non-physiological constraints that MT faces. Recent work by Girard et al. (2017) improves on ihMT for SC applications by removing CSF pulsation artifacts and showing that ihMT-weighted contrast can be obtained in an approachable scan time. Zhang et al. (2019) reviewed preclinical and validation studies of ihMT and showed good intra- and inter-scanner reproducibility *in vivo* in human cerebral WM tract; further development and validation are

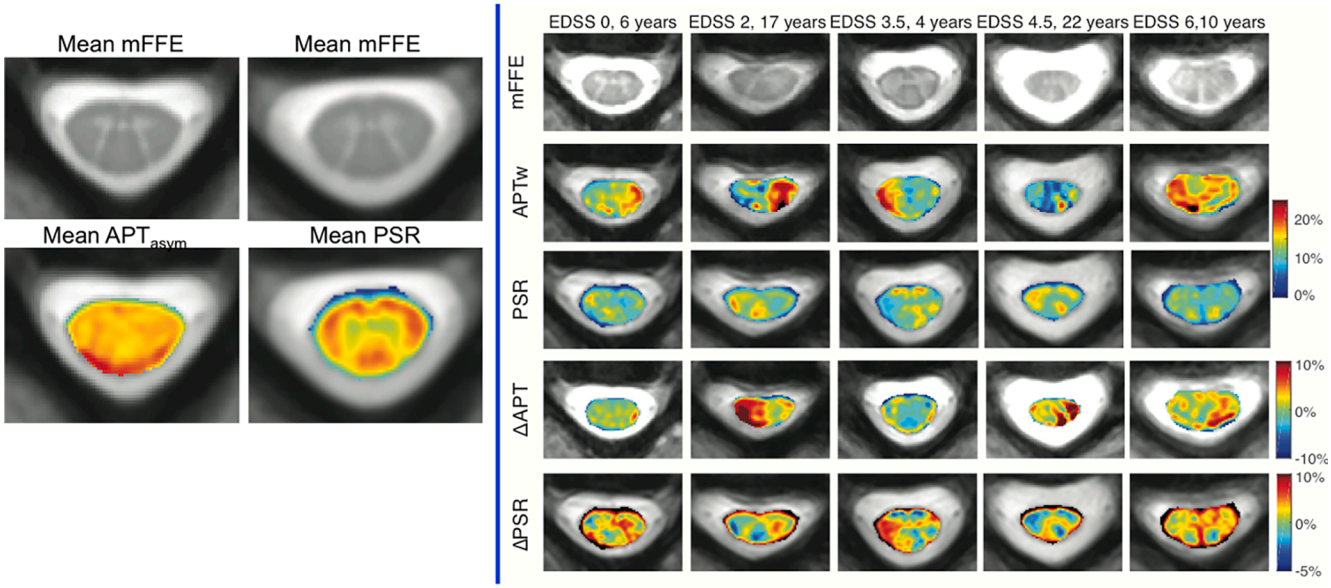

Fig. 1. Left: mean anatomical mFFE, APT_{asym} and PSR for five healthy controls obtained at 3T. Note the high contrast between the internal gray matter and surrounding white matter for the mFFE acquisition. Right: single-subject mFFE, APT_{asym}, PSR (top three rows) for five pwMS. An increase in the APT signal, and a concomitant decrease in the PSR are seen where lesions are identified on the mFFE. The bottom two rows shows ΔAPT and ΔPSR, or the difference of the APT_{asym} and PSR in each patient from the average healthy control image shown on the left panel. This calculation highlights the areas within the spinal cord that are distinct from healthy controls, and shows the potential contrast that could be used to study MS pathology over time. APT = Amide Proton Transfer; mFFE = multi-echo Fast Field Echo; PSR = Pool Size Ratio.

underway (Cohen-Adad, 2018). Lastly, Rasoanandrianina et al. (2020) showed that ihMTR was significantly different in the SC of pwMS compared to controls, and that ihMTR showed higher sensitivity to those changes than DTI or MTR metrics. This first study applying ihMTR to the MS SC is promising, and future studies should test the reproducibility of these findings.

2.1.3. Chemical exchange saturation transfer

Chemical Exchange Saturation Transfer (CEST) is similar in procedure to MT and ihMT, but distinct in its contrast mechanism. CEST contrast is generated by the transfer of spectrally specific RF saturation from labile protons and the surrounding water through direct chemical exchange rather than dipole–dipole interactions as is seen for MT. CEST is sensitive to small, mobile molecules that have exchangeable protons resonating at frequencies sufficiently distinct from water, exchange rates on the slow to intermediate time scales, and in sufficient abundance. The most common CEST method is Amide Proton Transfer (APT) which has been studied extensively in cerebral ischemia (Sun et al., 2007) and stroke (Msayib et al., 2019), and cancer. APT has been shown to be sensitive to proteins and peptides through the amide protons of the protein backbone and reflects changes in pH and protein concentration (Van Zijl and Yadav, 2011). APT-CEST in the CSC has been shown to be altered in pwMS compared to healthy controls (By et al., 2018a; Dula et al., 2016a), demonstrating potential for a new contrast mechanism in the SC. APT-CEST could be sensitive to increases in proteins/peptides observed during neuroinflammation processes underlying MS pathology.

Another advantage of CEST is that it can be 'tuned' to be sensitive to other metabolites or molecules of interest. Kogan et al. (2013) showed that glutamate sensitive CEST (GluCEST) can be obtained in the SC at 7 Tesla (T), opening opportunities to study neurotransmission and toxicity.

Even though there is a wealth of CEST opportunities in the MRI community, the vast majority have not been translated to the SC due to the long acquisition times, sensitivity to B_1 and B_0 effects, and relatively low sensitivity to its measurement targets. Providing a contrast mechanism that is sensitive to neuroinflammation, neurotransmitter aberrations, pH, or other progenitors of MS disease evolution would be highly desirable. Technical advancements, simulation, validation, reproducibility studies and evaluation of sensitivity and specificity for SC applications remain on the horizon.

2.2. Functional, metabolic, and vascular measures

2.2.1. Functional MRI

Task-based and resting-state functional MRI (fMRI) studies have shown the complex effects of MS on the brain's functional architecture and its evolution over the course of the disease; they can be explored in the CSC and have seen a few applications in MS research.

Previous block-design studies employing a tactile stimulation paradigm showed increased activation and alterations in recruitment patterns in the CSC in pwRRMS, compared to controls (Agosta et al., 2008a, 2008b; Valsasina et al., 2012), which also correlated with disability status (Valsasina et al., 2010). A related study provided preliminary evidence that neural correlates of MS-related fatigue may be measured in the CSC: the spatial extent of recruitment during tactile stimulation was greater in fatigued vs non-fatigued pwRRMS (Rocca et al., 2012). With newer acquisition schemes in the transverse plane and improved spatial resolution, GM horns can now be visualized axially, and the resting-state functional connectivity properties of the CSC in healthy volunteers have been described (Barry et al., 2016, 2014; Kong et al., 2014). One resting-state fMRI study of the CSC at 7T found no global differences in functional connectivity between pwMS and controls using a region-pair seed-based approach. WM lesions were found to have complex effects, causing both increases and decreases in connectivity metrics on different within-segment same-level functional networks depending on their location in different tracts and whether up- or downstream of the GM networks of interest (Conrad et al., 2018). Another study at 3T observed a link between increased resting-state connectivity in the CSC sensory network in pwRRMS and greater tissue damage as measured by DTI, suggesting that functional compensatory mechanisms may exist in the cord similarly to those observed in the brain in the early disease stages (Combes et al., 2022).

Further clinical applications will be facilitated as advances in

acquisition (Barry et al., 2018a; Kinany et al., 2022), quality assessment and pre-processing (Eippert et al., 2017) are made. The use of 7T can benefit SC fMRI via increased sensitivity to susceptibility effects for BOLD effect-based (T_2*) contrast, and greater SNR which enables acquisitions with sub-millimeter in-plane resolution. In the research setting, higher spatial resolution may prove useful to help reduce partial volume effects and, ideally, examine activity in specific neuronal populations underlying motor and sensory processing, including nociception (Kolesar et al., 2015). Data-driven methods like the Independent Component Analysis (ICA) can be used in the CSC (Kong et al., 2014) and may be applied to study GM circuits in the MS cord. An illustration of the main methods for analyzing SC resting-state fMRI data is shown in Fig. 2.

While theoretical and methodological validation is a complex issue, knowledge can be gained from the extensive research field of brain fMRI, and preclinical work in non-human primates that allows for simultaneous electrophysiological recordings to validate the origins and properties of the fMRI signal in the SC (Wu et al., 2019). Other existing methods developed for functional imaging of the brain may be applied in the future, including but not limited to exploring the features of the hemodynamic response function in the cord, fMRI of the WM which could reveal information on the functional properties of affected tracts, and dynamic connectivity approaches (Kinany et al., 2020). The development of simultaneous brain and CSC fMRI protocols (Cohen-Adad et al., 2010; Finsterbusch et al., 2013; Islam et al., 2019) may also enable investigations of cortico-spinal activity at rest and during motor or sensory tasks, which may be of value when studying impairments in sensorimotor function (Vahdat et al., 2020), nociception and neurogenic pain mechanisms (Tinnermann et al., 2021), and functional plasticity across the neuraxis. Finally, a few investigations have reported

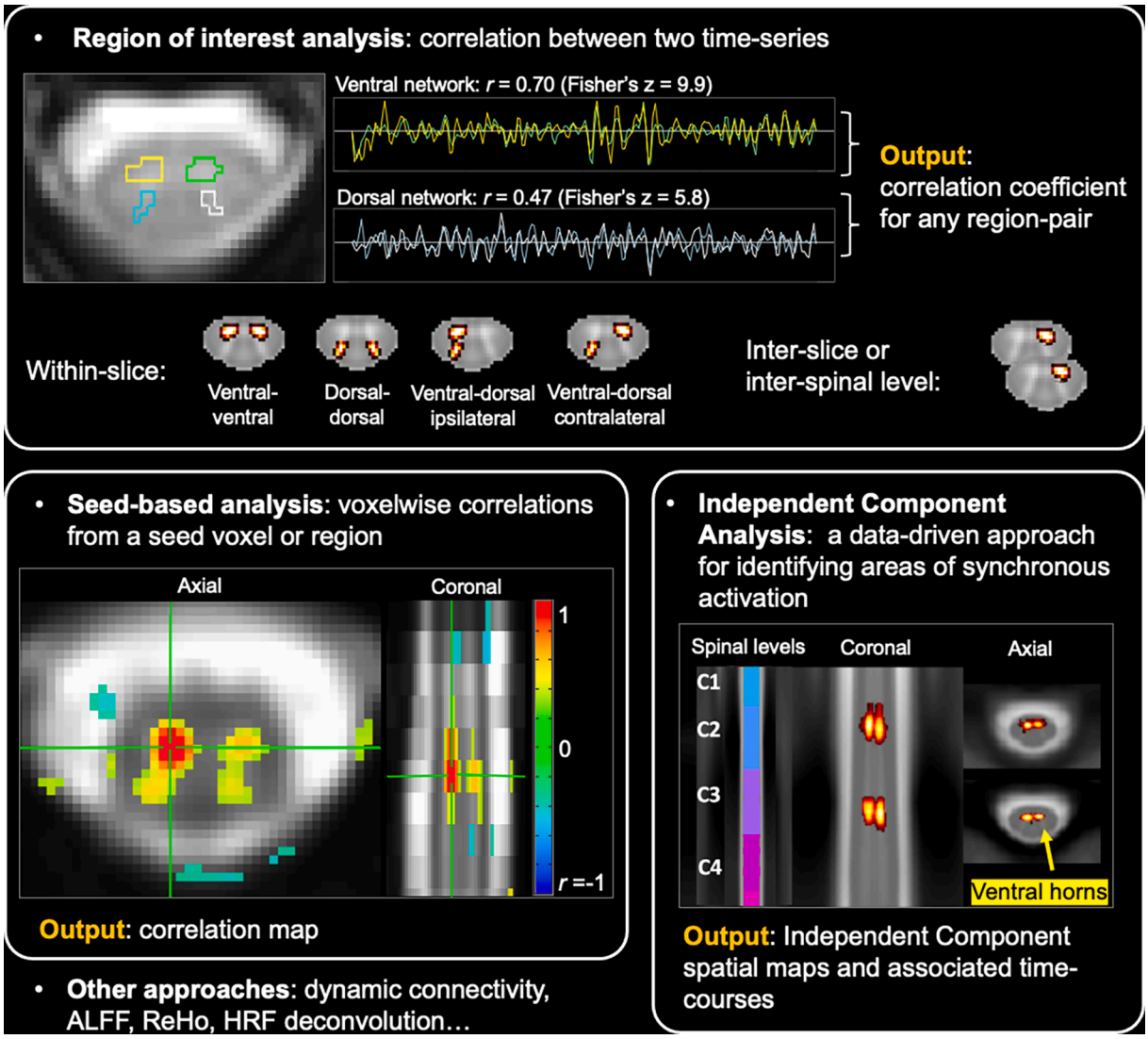

Fig. 2. Illustration of the main post-processing methods for resting-state functional MRI of the spinal cord. Example outputs are shown for region of interest-based, seed-based, and Independent Component (ICA) analyses. ROI analysis: a single axial slice showing regions of interest in the four grey matter horns and corresponding extracted time-series. Correlations can be computed between any two time-series, giving a coefficient as an outcome measure of functional connectivity. Those measures can be obtained between any two regions within or across slices or spinal levels. Seed-based analysis: example of a single-subject exploratory analysis, showing positive and negative voxelwise correlations (thresholded at $r < -0.25$ and $r > 0.25$), with a seed voxel placed in the anterior grey matter horn shown with green crosshairs. Correlated regions are seen by order of magnitude in the contralateral ventral horn, the ipsilateral dorsal horn, and the contralateral dorsal horn within-slice. ICA: two Independent Component maps corresponding to the ventral grey matter network at two spinal levels in the cervical cord are shown, derived from five subjects' data. Other approaches include dynamic connectivity methods, amplitude of low frequency fluctuations (ALFF), regional homogeneity analysis (ReHo), haemodynamic response function (HRF) deconvolution, and among others. (For interpretation of the references to colour in this figure legend, the reader is referred to the web version of this article.)

moderate-to-good within-session reproducibility of ventral and dorsal networks functional connectivity (Barry et al., 2016; Hu et al., 2018), as well as consistency between acquisition methods (Kinany et al., 2022) and across studies, which lends credibility to SC fMRI as a research tool, although more test–retest and longitudinal studies are required.

2.2.2. MR spectroscopy and sodium imaging

Proton magnetic resonance spectroscopy (MRS) allows for the *in vivo* quantification of several metabolites reflecting neural and glial function, some of which are thought to be implicated in MS pathophysiology. Moccia and Ciccarelli (2017) provide an extensive discussion of the applications of MRS to study brain and SC tissue in MS, organized by metabolite. Swanberg et al. (2019) review the influence of various methodological factors at play in MRS studies of MS, from study design to metabolite estimation. More specifically, studies using MRS in the CSC in MS are briefly discussed by Basha et al. (2018) and further reviewed by Chen et al. (2020); overall, reduced levels of *N*-acetyl aspartate and increased myo-inositol can be found in pwMS, are generally correlated with EDSS but not with cross-sectional area (CSA). The particular obstacles to SC MRS include the necessity for adequate B_0 shimming, and the inherent low spatial resolution of the method preventing tissue type-specific measurement, which will need to be addressed before its clinical potential can be exploited.

One particularly promising application of MRS is sodium quantification. Sodium accumulation, via expansion of the extracellular space and metabolic disruption of axonal ion channels, may be a contributing factor for neurodegeneration in MS (Huhn et al., 2019). Sodium imaging has been adapted for use in the CSC using MRS and a reference phantom (Solanky et al., 2013). Solanky et al. (2020) used ^{23}Na-MRS at 3T in the CSC in pwRRMS compared with controls and found an increase in total sodium concentration (TSC) controlling for demographic factors and independently of CSA. TSC was correlated with whole-cord (GM and WM, including lesioned tissue) FA in pwMS, and associations were noted with mediolateral postural stability, albeit in a small sample. The large effect size of the group comparison and observed relationship of TSC with microstructural WM damage, as measured with DWI, is promising given the biological specificity of this method and its high reproducibility in healthy controls (Solanky et al., 2013). However, it also appears to have a relatively high data quality rejection rate which should be addressed in future studies.

2.2.3. Susceptibility imaging

The central vein sign (CVS), i.e. the presence of a visible central vein on T_2*-weighted imaging or susceptibility-weighted imaging (SWI), can be identified in cerebral WM T_2 lesions. Histopathological reports of the CVS exist since some of the earlier descriptions of MS (Dawson, 1916), and it has been proposed as a robust imaging marker capable of differentiating between MS and other conditions with high sensitivity and specificity (Sati et al., 2016; Sinnecker et al., 2019). With MS having a heterogeneous clinical and radiological presentation and many "mimics", the value of identifying the CVS to aid the diagnosis of MS in and beyond the brain represents an attractive research goal with evident clinical utility. In the brain, the CVS has been studied across all scanning platforms, susceptibility-weighted protocols and field strengths demonstrating its potential usefulness in a diagnostic setting (Samaraweera et al., 2017; Sati et al., 2016; Sinnecker et al., 2019). Possible lines of investigation on the 'hunt' for the CVS in the SC include using high-resolution, high-field T_2*-weighted imaging, SWI, and the potential use of a contrast agent (see Chen et al., 2020). Encouragingly, one group recently showed the feasibility of imaging the CVS in upper CSC inflammatory lesions in patients with MS and other conditions, using a SWI protocol with a head coil at 3T (Jensen-Kondering et al., 2022).

An extension of SWI is quantitative susceptibility mapping (QSM). Although QSM is sensitive to iron and myelin content, the most pertinent application in MS may be the identification of paramagnetic rim lesions, a subset of chronic active brain lesions identified on SWI as having a paramagnetic rim. These lesions, characterized by demyelination within the lesion's core and a rim of iron-laden macrophages and microglia on the lesion's edge (Bagnato et al., 2011), tend to fail to repair, slowly expand over time and, similarly to the CVS, may have potential diagnostic applications (Absinta et al., 2016; Clarke et al., 2020; Dal-Bianco et al., 2017). However, there are so far no applications of SWI or QSM in the MS cord, making this an exciting target for future developments.

2.2.4. Perfusion

Implementation of perfusion measures in the cord without exogenous contrast agents has been challenging (Lévy et al., 2020). While some headway has been made with regards to the pathological origins and clinical value of perfusion measures in MS (Granziera et al., 2021; Lapointe et al., 2018), its merit in the cord for the study of MS remains to be ascertained.

3. Avenues for future research

3.1. Better measures of gray matter pathology

GM damage in the SC, as measured by atrophy and presence or extension of lesions into the GM, is an independent determinant of clinical status and disability (Bonacchi et al., 2020; Kearney et al., 2015; Schlaeger et al., 2015). Isolation and quantification of GM damage is, however, currently lacking as most sequences are tailored for the assessment of WM pathology; thus, more sensitive and specific measures are much needed.

SC GM area is best measured on T_1-weighted phase-sensitive inversion recovery (PSIR; Papinutto et al., 2015; Schlaeger et al., 2015, 2014) or gradient-echo T_2*-weighted axial images, both of which provide good GM/WM contrast. Recent work comparing different sequences and field strengths for GM visualization (Cohen-Adad et al., 2022; Papinutto and Henry, 2019), as well as a framework for the quantitative evaluation thereof, paves the way for further development of better SC GM structural imaging.

There are, to the authors' knowledge, no reports of regional SC GM atrophy in MS beyond looking at GM and WM compartments. Assessment of regional atrophy (e.g. different horns) would, in theory, be made possible with higher spatial resolution acquisitions, scans with improved GM:WM contrast, and using standard space atlases. Voxel-wise mapping methods have already been used to assess whole-cord atrophy (Freund et al., 2022; Valsasina et al., 2013). Another candidate is tensor-based morphometry, a method based on extracting the Jacobian matrix of the warp fields to a template space, which has been used to look at cord and GM regional volumes between younger and older healthy adults (Taso et al., 2015).

Relatively little attention has been paid to lesion identification in the GM specifically, although GM lesion load in the CSC has been estimated as only 28 % smaller than in the WM for RRMS, and that difference is even smaller in progressive subtypes (Eden et al., 2019). Current imaging techniques capable of identifying GM-only lesions, as opposed to WM or mixed WM/GM lesions, are lacking, despite their presence being known from histopathology (Gilmore et al., 2006). Among available sequences, 3D T_1-weighted PSIR (Fechner et al., 2019; Mirafzal et al., 2020) and proton density/T_2*-weighted gradient-echo (Fast Field Echo sequences; MERGE/MEDIC) are best suited for lesion identification, although those have not yet been adopted into clinical practice. Other proposed methods are discussed in Moccia et al. (2019), who also note the lack of sequences optimized for GM lesion identification.

SC lesions often extend across the WM/GM boundary and have 'blurry' edges. Furthermore, lesion intensity on T_2*-weighted images is similar to that of GM and so differentiating healthy-appearing from lesioned GM tissue is not an easy task, even when performed by experienced raters. Lesions may also confound the measurement of GM area in cases where it may have been a clinically pertinent marker (Sastre-Garriga et al., 2022a). The CNN lesion detection algorithm proposed by

Gros et al. (2019) has *a priori* knowledge of the healthy GM contour; however, the accuracy of automated lesion segmentation in WM vs GM was not assessed in this study. Future proposed developments include making use of different image contrasts when available, and including measures of lesion delineation uncertainty to prompt human intervention in particular cases (Gros et al., 2019).

GM demyelination has been measured in the normal-appearing cortex and cerebral deep GM structures, with the former being particularly clinically relevant; pathology studies have shown that cervical GM demyelination is as severe as that seen in cortical GM (Gilmore et al., 2009). However, *in vivo* SC MR methods with sensitivity to GM pathology beyond gross atrophy and lesion load are limited. Loss of axonal density, neuronal shrinkage and loss may also be present and may contribute to GM atrophy (Schmierer et al., 2018).

Quantitative T_1 mapping has high sensitivity but low specificity to pathological changes in general; however, its relative ease of acquisition and processing make it an attractive option. Dvorak et al. (2019) found similar MWF but higher T_1 in the SC GM of one pwRRMS. High-resolution T_1 mapping may hold promise for resolving fine anatomy of GM sub-regions (Massire et al., 2020), and quantifying and tracking changes in tissue over time.

The T_1-weighted/T_2-weighted ratio measurement has been proposed for evaluating cortical myelination from standard T_1- and T_2-weighted scans. The pros (Nakamura et al., 2022) and cons (Mühlau, 2022) of construing this measure as an indicator of myelin content have been debated. To the authors' knowledge, those measures have only been tested once in the SC of a single younger pwMS with a relatively short disease duration, compared to a range of control values, showing qualitative difference in lesioned tissue, but not in normal-appearing GM (Teraguchi et al., 2014).

Sequences designed to evaluate WM damage may be applied in the GM, although they typically suffer from reduced SNR. MWF measurements have lower accuracy and reliability in the GM, since myelin content is lower (Lee et al., 2020; MacKay and Laule, 2016). The macromolecular proton fraction from single-point qMT imaging showed acceptable test–retest reliability in the GM (Smith et al., 2014), although further work is needed to determine whether those methods have enough sensitivity to detect non-lesional myelin loss in the SC GM. Advanced diffusion models (e.g. NODDI, diffusion kurtosis imaging) may also find applications in the GM to study microstructural tissue properties other than myelination, such as various aspects of neurite morphology. Particularly promising, the NDI showed differences between pwMS and controls in CSC normal-appearing GM (By et al., 2017) and normal-appearing WM (Collorone et al., 2020), although normal-appearing tissue differences have not yet been corroborated by pathology (Grussu et al., 2017), and potential confounding factors may require further investigation. For overviews of the application of DWI models to MS pathology, including in the SC, see Cercignani and Wheeler-Kingshott (2019) and Lakhani et al. (2020).

3.2. Beyond the cervical spinal cord

While the CSC is a site of high disease activity in MS (Ouellette et al., 2020b), and has shown most improvement in advanced MRI methods, imaging of other cord areas is even less developed and further complicated by proximity to bone, heart and lungs, greater B_0 field inhomogeneity, and the lack of dedicated hardware. In this section, general considerations regarding MRI of the cervical and thoracolumbar spine, integration of brain and CSC imaging, and imaging of the peripheral nervous system (PNS) in MS are discussed.

3.2.1. Optimizing CSC coverage

Advanced MR scans in the CSC are most often done in the transverse plane to highlight intra-cord anatomies, sometimes limiting coverage in the rostro-caudal direction. Acquisitions with smaller fields of view are usually centered above the cervical enlargement, which offers several anatomical advantages: a straighter segment of the cord, less motion, and predominate location of MS lesions (Eden et al., 2019). Below C5, issues of B_0 inhomogeneity and motion related to proximity to the heart and lungs arise, often leading to lower data quality in those segments (Massire et al., 2018a). This, in turn, can confound results, for instance, in correctly identifying lesions (e.g. Kerbrat et al., 2020).

The mobility and curvature of the cord in the CSC present a particular challenge. The use of several stacks to roughly align with the cord (for an example, see Ouellette et al., 2020) may be valuable at the expense of increased acquisition times and more elaborate manual intervention during scan pre-planning. Another approach is using a multi-slice-multi-angle (MSMA) strategy, enabling transverse acquisition of several slices orthogonally to the curvature of the cord at different angles each. This configuration aims to limit partial volume effects and allows for a more accurate representation of anatomy, in less time than the acquisition of multiple stacks. Massire et al. (2018b) demonstrated feasibility of a DWI sequence using MSMA at 7T (~6 min for 7 mid-vertebral slices from C1 to C7) and showed good reproducibility of the obtained indices. There are currently no studies evaluating the benefit, if any, of such acquisition schemes compared to typical ones for lesion detection or repeatability of imaging metrics in MS.

3.2.2. Brain and cord imaging

Concurrent brain and cord imaging studies are surprisingly scarce, likely resulting from the associated time constraints as well as the relative lack of maturity of advanced SC imaging methods. Most of these studies only include cord involvement as a binary 'yes/no' measure, or summary measures of CSC area and/or lesion load, since the scans are often included in clinical work-up. Several studies found that upper CSC area is the strongest predictor of EDSS (Song et al., 2020), particularly in progressive subtypes (Furby et al., 2008; Ingle et al., 2003) and patients with longer disease duration (Daams et al., 2014). Cord atrophy is also generally unrelated to global brain atrophy (A. B. Cohen et al., 2012; Ingle et al., 2003; Ruggieri et al., 2015). This suggests that pathology in those compartments progresses at least partially independently; those observations make a case for imaging both structures, and for the CSC area to be included in 'composite measures of neurodegeneration' (Furby et al., 2008). However, a more refined look into regional GM in relation to upper CSC area revealed relationships with infratentorial volumes (Bellenberg et al., 2015). Imaging of GM structures, WM tracts, and regional volumes in both brain and cord would help describe both independent and related (e.g. via Wallerian degeneration) measures of CNS damage across the neuraxis.

In the spirit of leveraging brain datasets to include upper CSC atrophy measures, several groups have looked into quantifying cord atrophy from routinely acquired brain scans (Liu et al., 2016, 2015; Lukas et al., 2021; Papinutto et al., 2018; Taheri et al., 2022). Bischof et al. (2022) inspected cord atrophy in a large legacy dataset of over 400 progressive pwMS with a 12-year follow-up, looking at C1 area in relation to disease progression trajectories, and showing that an accelerated atrophy rate in RRMS before conversion to secondary progressive (SP) disease. Freund et al. (2022) used the BSC-SPM framework (see 'Analysis tools' section) to perform voxel-based morphometry (VBM) in the brain and CSC of pwMS and controls, showing feasibility of a unified analysis pipeline for concurrent assessment of regional brain and cord atrophy on T_1-weighted MPRAGE images using a template extending to the upper CSC.

Yet, few studies have used advanced methods to look at tissue damage beyond simple measures of lesion load in both brain and SC. Using the ICBM152 brain and PAM50 cord templates (both in MNI space) and an automated SCT-based pipeline, Kerbrat et al. (2020) performed voxelwise lesion mapping in the cortico-spinal tract (CST) from brain to cervical cord in 290 pwMS from 8 centers, and examined lesion distribution along the whole CST, the impact of CST lesion load and location on disability, and the predictive power of those measures for disability progression at two years. Ouellette et al. (2020) observed the spatial distribution of lesions in the brain and entire CSC in RR and

SPMS participants, taking advantage of the greater spatial resolution, SNR and CNR afforded at 7T, although the brain and SC protocols were acquired separately. Weber et al. (2022) found greater CSC atrophy and lesion load in pwRRMS with brain iron rim lesions, compared to those without.

Beyond structural and lesion load measures, Vaithianathar et al. (2003) looked at T_1 in the CSC, brain GM and WM in pwMS, and found that in addition to T_1 differentiating between subtypes, cord and cerebral WM T_1 were related, suggesting that secondary degeneration processes may underlie this relationship. In a series of investigations, Rovaris et al. used atrophy and MTR measures in both CSC and brain in participants with primary progressive (PP) MS, finding no correlations between the two, but confirming a role of cord CSA in explaining disability separately from brain measures, and thus confirming those measures as complementary (Rovaris et al., 2008, 2001, 2000). Filippi et al. (2002) also found correlations between MTR in the CSC, and fMRI measures of cerebellar activation during a motor task in pwPPMS. Kolind et al. (2015) used brain and cervical cord MWI to assess atrophy and demyelination in relation to clinical indices in a PPMS group. Lema et al. (2016) found that median whole-brain MTsat and peak whole-cord MTsat were correlated at the trend level, controlling for age. Collorone et al. (2020) applied whole-brain and CSC NODDI, and found that cord metrics showed stronger correlations with EDSS, although relationships between brain and spine metrics were not assessed. Bonacchi et al. (2020) investigated 120 pwMS with structural brain and CSC measures, in addition to diffusion-weighted imaging (DWI) in the cord, and identified CSC measures (CSC GM lesion load, GM atrophy, and lateral funiculi FA) as the most relevant variables for explaining EDSS scores, and differentiating relapsing vs progressive pwMS in multivariate analyses that included volumetric brain measures. Taken together, these studies suggest that brain and CSC damage provide complementary information that help explain disease status and prognosis. Multiparametric assessments may be valuable in identifying the relative contributions of brain and cord parameters in explaining and predicting disease status, and thus identifying the best markers of disease progression, conversion to progressive disease, and measuring neuroprotective effects of therapies in clinical trials.

Further advancements are also making possible the simultaneous acquisition of brain and cord data (for discussion of brain-cord functional MRI, see 'Functional MRI' section). Cohen-Adad (2021) presented an application of the SIEMENS syngo-RESOLVE ("readout segmentation of long variable echo-trains") sequence to image brain and CSC concurrently, enabling high-resolution (2.2 mm isotropic) tractography; this acquisition was possible at 3T with b = 800 s/mm^2 and 30 diffusion-weighted directions in <11 min. An example of DTI-based tractography from the cortex to the CSC, which would be useful to map and assess the integrity of cerebrospinal WM pathways, is shown in Fig. 3. Forodighasemabadi et al. (2021) developed a combined brain and whole cervical MP2RAGE acquisition with sub-millimeter resolution in <8 min, with particular attention to mitigating B_1^+ inhomogeneity, enabling anatomical and segmentation and quantification of T_1 in the main CSC WM tracts as well as brain regions of interest with high scan-rescan reproducibility. Finally, with regards to data processing, the SPM-BSC currently only includes the upper four cervical levels, although future extension to the whole CSC is planned (Freund et al., 2022). The presently available PAM50 template is also compatible with the MNI coordinate system, awaiting further applications in simultaneous or concurrent brain/cord imaging.

3.2.3. *Thoracolumbar imaging*

While SC motion is less prominent in lower-thoracic and lumbar segments relative to cervical and upper-thoracic segments (Figley et al., 2008), imaging the thoracolumbar SC is subject to other challenges including its smaller size (~1 cm), pulsating CSF flow, position within large bones (B_0 inhomogeneity), temporally varying B_0 inhomogeneity due to respiration, and wrap artefacts from the torso. In comparison to the CSC, the thoracolumbar SC remains understudied with MRI, in part due to these challenges, even though thoracolumbar lesions were found in 41 % of patients in a heterogeneous MS cohort, albeit less frequently than cervical lesions (Weier et al., 2012) (see Fig. 4). However, the presence of thoracic lesions can be predicted by CSC lesion load, and thus, assuming similar pathological mechanisms in the thoracic, compared to other portions of the cord, it has been suggested that there may be limited added value in further advanced imaging of the thoracic portions (Hua et al., 2015).

Cord atrophy is consistently more pronounced in cervical than thoracic regions. Mina et al. (2021) hypothesized this could be owing to either limitations of imaging sequences, or a "floor effect", i.e. a lesser capacity for tissue loss given the smaller starting volume of the thoracic cord. Thoracic volume was unrelated to brain and cervical atrophy measures in a mildly impaired RRMS group, and was not correlated with clinical indices (EDSS and T25FW) (Cohen et al., 2012). However,

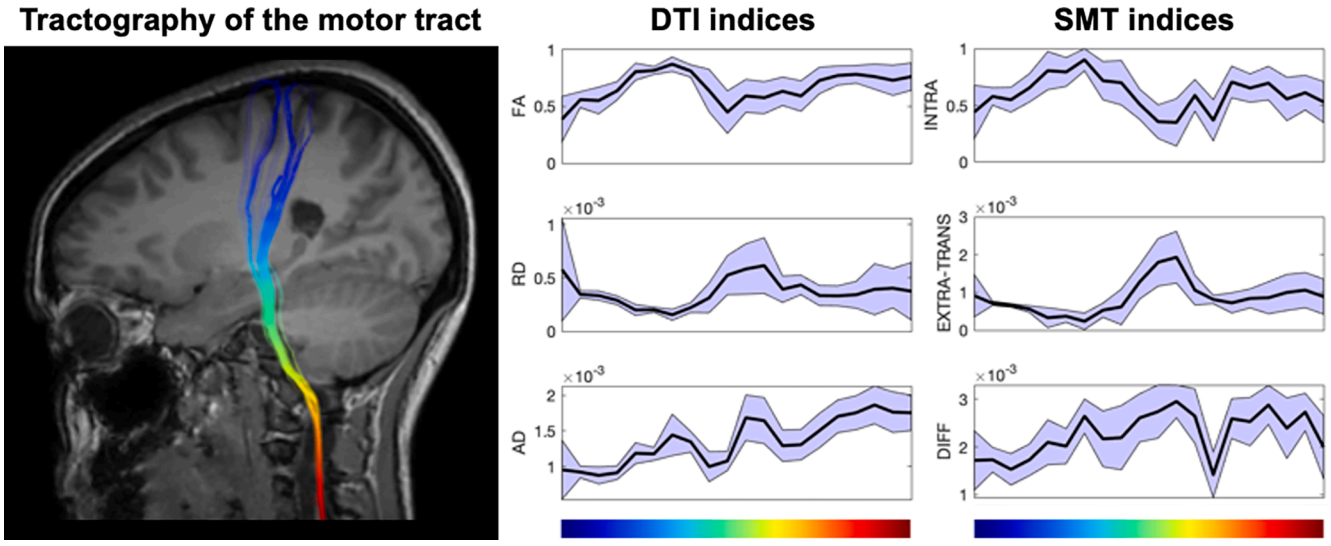

Fig. 3. Single-subject tractography of the motor tract from cortex to upper cervical cord, constructed by combination of separate brain and cervical cord acquisitions in a healthy volunteer at 3T. Variations in Diffusion Tensor Imaging (DTI) and Spherical Mean Technique (SMT) multi-compartmental modeling are shown along the tract. FA = Fractional Anisotropy, RD = Radial Diffusivity, AD = Axial Diffusivity, INTRA = intra-neurite volume fraction, EXTRA-TRANS = transverse microscopic diffusivity of the extra-neurite compartment, DIFF = tissue intrinsic diffusivity.

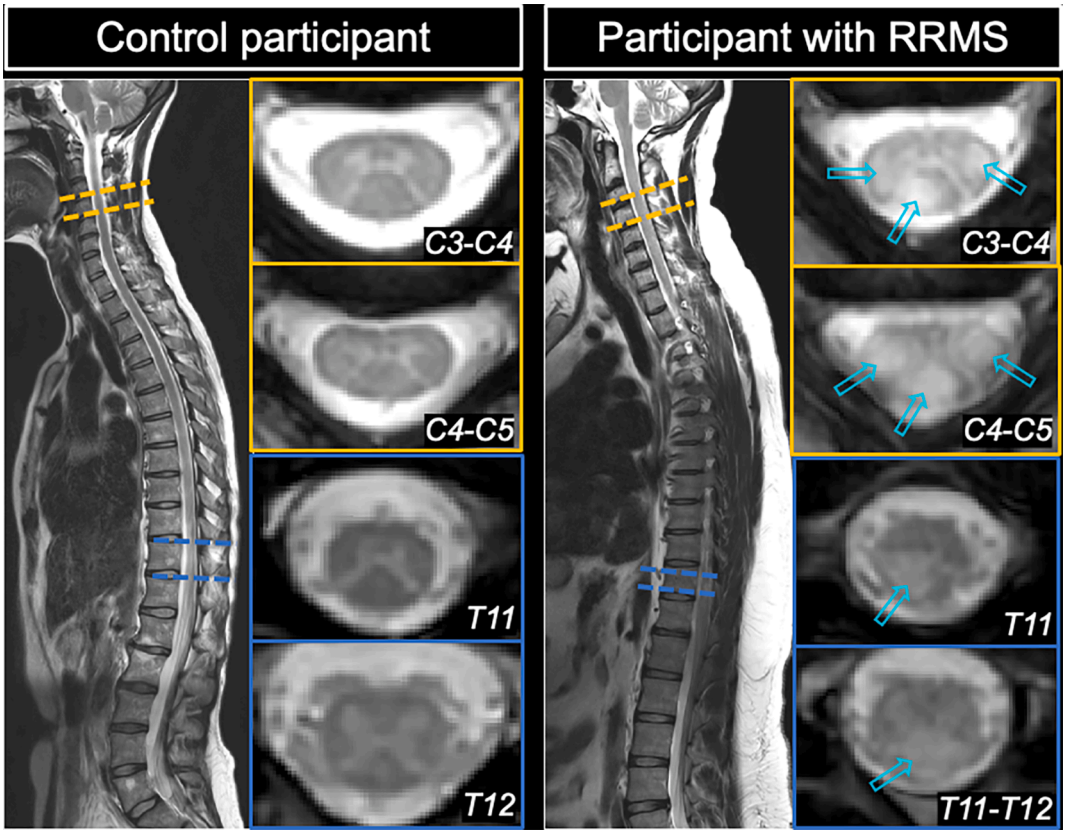

Fig. 4. Example sagittal T_2-weighted turbo spin echo and axial multi-echo fast field echo acquisitions at 3T for the cervical and lumbar spinal cord. Shown are one control (48-year-old female) and one participant with RRMS (35-year-old male, disease duration < 2 years, EDSS = 0). Cervical and lumbar scans were acquired separately. Blue arrows point to lesions on the patient scan, illustrating disease burden across two locations of the central nervous system. (For interpretation of the references to colour in this figure legend, the reader is referred to the web version of this article.)

inclusion of thoracic metrics was shown in a larger, more heterogeneous sample to improve grouping of patient phenotypes and correlations with clinical disability (Mina et al., 2021). Moreover, Schlaeger et al. (2015) showed that GM area at the T8-T9 level contributed to predicting EDSS score, independently of CSC CSA.

Those findings for lesions and atrophy may point towards the CSC as the more advantageous target for further investigation, at least for some purposes (e.g. biomarker development for clinical trials), and imaging of the thoracic and lower sections is currently not recommended for diagnosis, unless symptoms suggest involvement of those regions; if feasible, the upper thoracic region should be prioritized (Filippi et al., 2019; Traboulsee et al., 2016; Wattjes et al., 2021). There is however a dearth of advanced MRI studies in the cord beyond the CSC, and the added value of thoracolumbar imaging may be underestimated due to the lack of sensitivity of the 'gross' summary methods currently used (atrophy and lesion load). Current advances in hardware and acquisition, including the use of UHF, may eventually be deployed for lower cervical and thoracic cord (Gass et al., 2015) to address this. Further, studying the lumbar cord may provide insight into the mechanisms behind prevalent symptoms including bladder, bowel, and sexual dysfunction due to disrupted autonomic pathways and lower limb dysfunction, which causes mild or greater gait disability in 59 % of patients by 10 years of disease duration (Kister et al., 2013). The greater prevalence of impaired gait relative to hand dysfunction (Kister et al., 2013) and the effects of these symptoms on quality of life for patients (e.g. at least 75 % of patients with MS experience bladder dysfunction; Browne et al., 2015) also highlight the need to optimize MRI methods for lower SC segments.

3.2.4. *Peripheral nervous system MRI*

There are few investigations of the PNS in MS using MRI. Jende et al. (2017) used MR neurography to highlight differences in proton spin density and T_2 relaxation time in peripheral nerve lesions in the lower limbs. However, subgroups of pwMS with and without SC lesions did not differ from each other, suggesting that peripheral inflammation or demyelination reflected by those parameters may be a co-occurring, but independent process; and that taking this damage into account may contribute to reduce discrepancies between imaging and clinical status. Boonsuth et al. (2021) found lower MTR values in the sciatic nerve, but not the lumbar plexus of an MS group, further pointing towards peripheral pathological co-demyelination, rather than Wallerian degeneration stemming from possible SC lesions. Future similar studies could be strengthened by employing MRN for nerve region delineation, MTR and DWI, and lumbar cord imaging. Imaging the PNS concurrently with the CNS could inform on the common or distinct pathophysiological mechanisms underlying demyelination in both compartments, and may also have implications for patient monitoring, as nerve tissue can be collected *in vivo* by biopsy (Oudejans et al., 2021).

3.3. *More and better data: from study design to analysis*

3.3.1. *Study design: validation, reproducibility and harmonization*

MRI markers capable of accurately quantifying demyelination and axonal damage have evident utility in research and clinical trials of MS; thus, there is great interest in *in vivo* histology (i.e. microstructural imaging with high biological specificity) as well as validation of existing methods based on comparison of MRI of *ex vivo* animal or human tissue with histology or other imaging methods. An extensive review by Cohen-Adad (2018) describes the principles of microstructural imaging

using MRI in the SC, and details methods for validation of MR methods that purport to characterize tissue microstructure, including the challenges inherent to validation methods themselves. Schmierer et al. (2018) review post-mortem MRI studies combined with histology in the MS cord specifically, highlighting the potential of combined histology/MRI studies. Van der Weijden et al. (2021) review validation of several myelin imaging methods including those discussed above (see 'Myelin imaging' section), with reference to both preclinical and post-mortem validation studies, and human brain and SC reproducibility studies.

As different modalities are sensitive to different aspects of pathology, many have made the case for multi-parametric studies and combination of several modalities for improved tissue characterization (Cohen-Adad, 2018; Lévy et al., 2018; van der Weijden et al., 2021). An example of a composite metric that can be obtained by combining two sequences is the g-ratio, or ratio of axonal to myelin sheath diameter. G-ratio-weighted maps have been obtained in the CSC by using two sequences and combining axon diameter and myelin density measurements from DWI and proton density-based imaging, respectively (Duval et al., 2017), pointing out some current hurdles to repeatability (Duval et al., 2018). In the context of multi-parametric studies, scan time can be maximized by devising multi-contrast acquisitions; one example was proposed by Grussu et al., using a unified read-out and including MT and T_1, with the advantage of providing quantitative maps in the same space in a single acquisition, and potential for increased inter-site reproducibility (Grussu et al., 2020).

A strength of the MS MRI research field is the existence of international collaborative initiatives (e.g. MAGNIMS, CMSC, NAIMS, MS-PATHS) that propose to pool resources, data and knowledge to tackle important research questions. Harmonization efforts are also being undertaken by the SC research community, with the recent proposal of a 'consensus' research acquisition protocol for the CSC, including guidelines for participant positioning and scan prescription (Cohen-Adad et al., 2021b). In the context of MS, valuable additions to this protocol may be sequences to improve lesion detection, such as a 3D T_1-weighted PSIR or a sagittal STIR image, as per MAGNIMS recommendations (Wattjes et al., 2021). The 3D MP2RAGE sequence has also been proposed to improve CSC lesion detection compared with a typical clinical work-up (Demortière et al., 2020), includes the brain in an acceptable scan time (7 min), and also produces a T_1 map, which has the benefit of high reliability and sensitivity to pathology. Future prospective studies, which would benefit from deployment across research centers, are required. In the authors' opinion, susceptibility-based sequences capable of revealing vascular features have the potential for clinical impact and may benefit from further investigation.

Such multi-site reproducibility studies are also necessary to establish robust research protocols, as are single-subject 'travelling-spine' reliability studies (Cohen-Adad et al., 2021a; Lukas et al., 2021). The obtention of well-validated, reliable MRI markers are, in turn, paramount in establishing well-powered and efficient longitudinal studies and clinical trials. Finally, open-access datasets (Cohen-Adad et al., 2021a; Lukas et al., 2021) enable development of analysis tools.

3.3.2. Analysis tools

The development of freely available analysis tools has been instrumental in propelling the advanced SC imaging research forward. Although not cost-free, the JIM software is widely used for semi-automated segmentation using an active surface model (Horsfield et al., 2010; https://www.xinapse.com/). The SCT (https://spinalcordtoolbox.com/) has become a reference in the field, and includes pre-processing, general structural image manipulation, segmentation as well as individual processing tools for DWI, MT and fMRI data, including a lesion segmentation tool (De Leener et al., 2017; Gros et al., 2019). Prados et al. (2017) presented several algorithms for CSC GM segmentation as part of a community challenge, including links and an open-access training dataset. Toolboxes have also been developed for spinal fMRI specifically: 'pyspinalfmri' (https://www.queensu.ca/academia/stromanlab/dr-patrick-stroman/fmri-analysis-software) and the Neptune Toolbox (https://www.fmriresearch.com/neptune-toolbox/).

Regarding common-space atlases, De Leener et al. (2018) reviewed previous initiatives in constructing (cervical) SC templates from smaller datasets, before introducing the more widely-used PAM50 template, which spans the whole SC in MNI space, is compatible with several contrasts, and includes vertebral and spinal levels, GM subregions and WM tracts (available within the SCT; the code for template generation is available at https://github.com/neuropoly/template/). Also in MNI space, the BSC template within the SPM framework (Azzarito et al., 2021; Blaiotta et al., 2018) covers the brain and the first four cervical segments, with seven tissue classes (GM, WM, CSF, fat, non-neural tissues, soft tissues, bone/air mixture). Liu et al. (2020a) proposed a MWF and geometric mean T_2 CSC atlas (8 slices at C2-C3) from 20 control participants' data, based on a GRASE sequence (available in PAM50 space at https://sourceforge.net/projects/mwi-spinal-cord-atlases/).

The availability of consensus protocols (Cohen-Adad et al., 2021b) and free analysis tools will facilitate multi-center studies, increasing participant numbers. While larger datasets pose their own challenges in term of data storage and handling, they are invaluable for answering clinical research questions (De Stefano et al., 2022). One example of the potential utility of advanced SC imaging tools is the implementation of the generalized boundary shift integral (GBSI) method for longitudinal atrophy assessment, which relies partly on SCT software, and has been shown to theoretically decrease the required sample size for a clinical trial in PPMS (Moccia et al., 2020). In another example, Eden et al. (2019) were able to recruit 642 pwMS across 13 sites (with varying protocols, vendors, and field strengths), and used an automatic SCT-based processing pipeline to perform voxelwise lesion mapping in the CSC. This study with a considerable sample size showed that the greatest lesion burden was found in pwMS with higher EDSS but shorter disease duration, i.e. an 'aggressive' disease course – an observation that contributes to our increased understanding of the disease.

3.3.3. Ultra-high field imaging

UHF imaging refers to scanner strengths beyond 3T, i.e. 7T (and theoretically above, although all research cited below was conducted at 7T). Higher field strength offers greater SNR, allowing for acquisitions with higher spatial resolution, which is especially useful for resolving the small size of the SC and minimizing partial volume effects between CSF, WM and GM. Drawbacks include increased sensitivity to physiological noise, and difficulty of clinical implementation due to increased safety requirements and the scarcity of commercially-available SC coils. Specific absorption rate limitations may also impede implementation of certain advanced techniques (e.g. MT-based methods that rely on high-power saturation pulses).

There are, so far, few investigations of the SC in MS at 7T. Dula et al. (2016b) showed that 7T CSC imaging improved detection of CSC lesions by 52 % compared to a clinical 3T protocol using sagittal T_2*-weighted, axial T_1-weighted and T_2*-weighted scans in 15 pwRRMS, and improved visualization of anatomical features such as nerve roots. An example of acquisitions at 3 and 7T in a control and two pwMS is shown in Fig. 5. They also showed a significant increase in SNR and in GM:WM contrast-to-noise ratio between a typical 3T multi-echo Fast Field Echo (FFE) and a 7T single-echo FFE scan. Ouellette et al. (2020) used 7T to investigate the spatial distribution of CSC lesions in RR and SPMS at high resolution (0.40x0.40x3 mm^3), demonstrating an "outside-in" gradient from outer subpial surface to central canal in RRMS, and following an inverse pattern in SPMS. Dula et al. (2016a) evaluated optimized pulse parameters and B_1^+ homogeneity for an amide proton transfer CEST sequence at 7T and showed broad differences in Z-spectra features in normal-appearing WM and lesioned tissue between pwMS and controls. Preliminary investigations have used 7T to demonstrate increased lesion conspicuity in the thoracic cord (Lefeuvre et al., 2016), anterior vein enlargement (Witt et al., 2019), as well as atrophic features and abnormal lesional tissue values using DTI and T_1 relaxometry (Massire

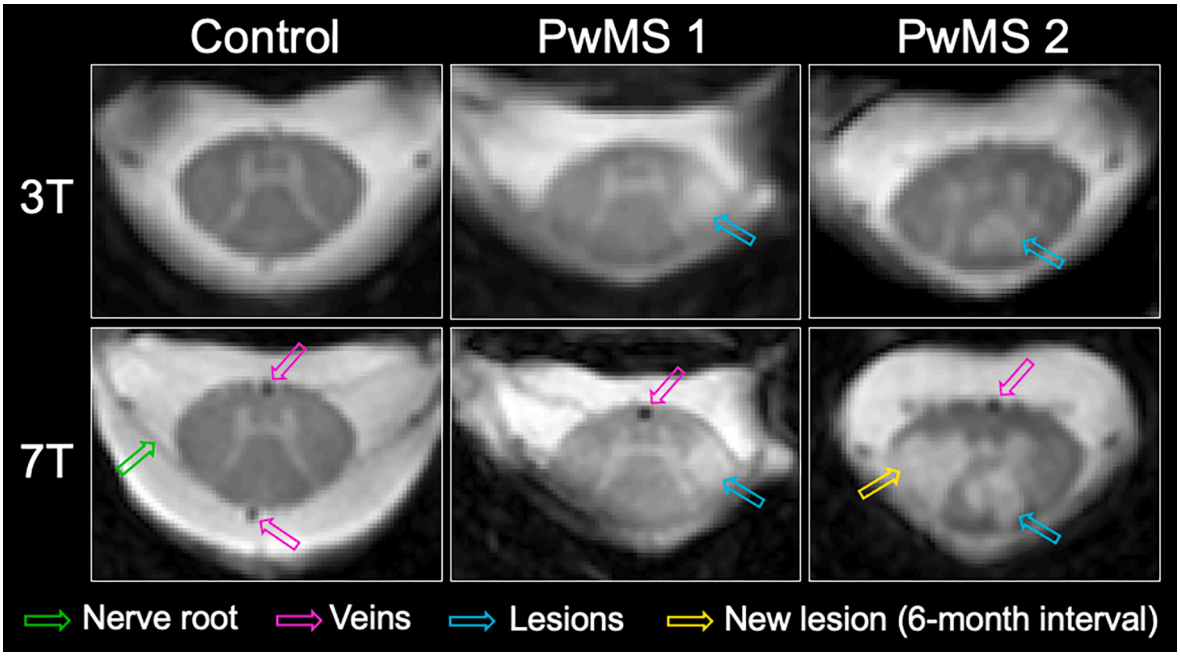

Fig. 5. T_2*-w multi-echo Fast Field Echo images in the cervical spinal cord at 3T (top row) and 7T (bottom row) in a healthy participant and two people with relapsing-remitting MS (pwMS). In the control participant (46-year-old female), greater anatomical detail is seen at 7T: nerve roots can be seen, and anterior and posterior spinal veins are more apparent. In pwMS 1 (35-year-old female, disease duration 1 year, EDSS 0), a lesion in the lateral column is seen at both field strengths; the anterior vein is visible at 7T. In pwMS 2 (35-year-old female, disease duration 1.5 year, EDSS 0), in the 7T scan which was acquired after a 6-month interval, a new lesion can be seen in the lateral column. Signal inhomogeneity within the dorsal lesion can be appreciated at 7T. The 'irregular' periphery of the cord reflects vasculature including the anterior vein. For both patients, while lesion conspicuity is comparable, more detail can be seen at higher field strength.

et al., 2019). Further investigations of the improved sensitivity of UHF for lesion detection in larger samples, across subtypes and lesion types, are needed to ascertain clinical utility, balanced against the challenges of UHF scanning in a medical setting. The higher spatial resolution and SNR achievable, and the greater sensitivity to susceptibility effects at 7T may prove useful for investigations requiring high-resolution anatomical imaging, fMRI, glutamate-CEST (Kogan et al., 2013), and susceptibility-based methods. There is, in theory, improved sensitivity to gadolinium contrast enhancement for lesion identification at 7T, which has not yet been formally investigated in the SC (Kreiter et al., 2022). For further reading, see Barry et al. (2018) for a technical overview of the advantages and challenges of 7T SC imaging, Ineichen et al. (2021) for advances in UHF applied to MS, and Kreiter et al. (2022) for a literature review on UHF MRI in the MS SC specifically.

3.3.4. *Applications of artificial intelligence*

Applications of artificial intelligence (AI) in brain MS research include aiding tissue class and lesion segmentation, patient classification (e.g. for differential diagnosis or between subtypes) and future disability and disease progression predictions; see reviews by Afzal et al. (2022) and Kontopodis et al. (2021). It stands to reason that similar methods may prove equally useful with SC data. AI is already used in processing tools: for automated segmentation of cord and CSF on T_1, T_2, T_2*, or diffusion-weighted images (Gros et al., 2019), and GM on T_2*-weighted images (Perone et al., 2018), both using neural networks within the SCT framework. A similar algorithm also exists within SCT for segmenting cord lesions on either sagittal or axial T_2-weighted scans (Gros et al., 2019). AI may further help with outstanding challenges in MS data analysis such as automated lesion identification, including using multi-contrast and longitudinal data (for tracking existing lesions and identifying new ones), and extracting information from large datasets. Deep learning may also assist in speeding up processing methods, such as CEST and fMRI, bringing them closer to being performed at the scanner or in clinic; an existing example is rapid MWI processing using a neural network (Liu et al., 2020b; see 'MWI' section above). Further applications may include patient classification (e.g. Toufani et al., 2021) and prediction of conversion to clinically-definite disease (Yoo et al., 2019), as have been more widely implemented in the brain.

4. Conclusion

Refinements in SC imaging were being identified 15 years ago as an important advancement in MS research, with the potential to clarify our understanding of the substrates of clinical disability (Bakshi et al., 2008). As reviewed herein, the field has made tremendous leaps in the last decade. From some of the first images showing the possibility of obtaining functional, macro- and microstructural images, to larger studies demonstrating the utility of these measurements in patient studies, it is evident that innovation and creativity from the SC imaging community have led to the development of instruments that can, and will continue to, increase our understanding of MS. As an example of success, the value of large-scale studies (e.g. Eden et al., 2019; Kerbrat et al., 2020) is clear, made possible by unified acquisition protocols, collaboration between centers, and semi-automated analysis tools.

However, even with the progresses made since then, the need for further and better imaging of the SC is still being recognized as crucial (Krieger, 2022). The big-picture opportunities for SC MRI in MS could be categorized in two arenas: 1) developing and utilizing fast, reliable imaging with high sensitivity and specificity, showing correlations with neurological status and relationships to evolving pathology, as presented here, to inform our understanding of the pathological mechanisms of MS and disease evolution; 2) addressing the relative stagnancy in the routine diagnostic portfolio. Indeed, as a counterpoint to the apparent improvements in advanced MRI, conventional SC MRI has not evolved nearly as much. The hope is that technical advancements gained from the research field may translate to clinical systems, by solving challenges related to anatomy, size, acquisition speed, etc. Examples include the advent of compressed sensing, AI-driven noise reduction, and continually improving coils and hardware. As we look forward, let us not forget to look side to side and recognize the need for improving

even the most basic sequences, as these can ultimately have the most direct clinical impact. As such, incremental improvements in diagnostic SC MRI should continue to be expected.

Finally, the advances discussed here for MRI of MS are also likely to see valuable applications in other inflammatory and/or neurodegenerative diseases affecting the SC, among which neuromyelitis optica spectrum disorder, MOG antibody-associated disease, transverse myelitis, and amyotrophic lateral sclerosis, where differential diagnosis, investigation of disease mechanisms, treatment efficacy monitoring and clinical trials all stand to benefit from advances in SC imaging.

CRediT authorship contribution statement

Anna J.E. Combes: Conceptualization, Writing – original draft, Writing – review & editing, Visualization. **Margareta A. Clarke:** Writing – original draft, Writing – review & editing. **Kristin P. O'Grady:** Writing – original draft, Writing – review & editing. **Kurt G. Schilling:** Writing – original draft, Visualization. **Seth A. Smith:** Conceptualization, Writing – original draft, Writing – review & editing.

Declaration of Competing Interest

The authors declare that they have no known competing financial interests or personal relationships that could have appeared to influence the work reported in this paper.

Acknowledgements

None.

Funding

Dr. O'Grady is supported by NIH/NIBIB award K01EB030039. Dr. Schilling is supported by NIH/NIBIB award 1K01EB032898. This work was supported by funding from the Conrad Hilton Foundation, National MS Society, and NIH/NINDS 5R01NS109114, 5R01NS117816 and 5R01NS104149.

References

Absinta, M., Sati, P., Schindler, M., Leibovitch, E.C., Ohayon, J., Wu, T., Meani, A., Filippi, M., Jacobson, S., Cortese, I.C.M., Reich, D.S., 2016. Persistent 7-tesla phase rim predicts poor outcome in new multiple sclerosis patient lesions. J. Clin. Invest. 126 (7), 2597–2609.

Afzal, H.M.R., Luo, S., Ramadan, S., Lechner-Scott, J., 2022. The emerging role of artificial intelligence in multiple sclerosis imaging. Mult. Scler. 28 (6), 849–858.

Agosta, F., Valsasina, P., Caputo, D., Stroman, P., Filippi, M., 2008a. Tactile-associated recruitment of the cervical cord is altered in patients with multiple sclerosis. Neuroimage 39, 1542–1548. https://doi.org/10.1016/j.neuroimage.2007.10.048.

Agosta, F., Valsasina, P., Rocca, M., Caputo, D., Sala, S., Judica, E., Stroman, P., Filippi, M., 2008b. Evidence for enhanced functional activity of cervical cord in relapsing multiple sclerosis. Magn. Reson. Med. 59, 1035–1042. https://doi.org/10.1002/mrm.21595.

Alexander, D.C., Hubbard, P.L., Hall, M.G., Moore, E.A., Ptito, M., Parker, G.J.M., Dyrby, T.B., 2010. Orientationally invariant indices of axon diameter and density from diffusion MRI. Neuroimage 52, 1374–1389. https://doi.org/10.1016/J.NEUROIMAGE.2010.05.043.

Alonso-Ortiz, E., Levesque, I.R., Pike, G.B., 2015. MRI-based myelin water imaging: a technical review. Magn. Reson. Med. 73, 70–81. https://doi.org/10.1002/mrm.25198.

Andersen, K.W., Lasič, S., Lundell, H., Nilsson, M., Topgaard, D., Sellebjerg, F., Szczepankiewicz, F., Siebner, H.R., Blinkenberg, M., Dyrby, T.B., 2020. Disentangling white-matter damage from physiological fibre orientation dispersion in multiple sclerosis. Brain Commun. 2 https://doi.org/10.1093/BRAINCOMMS/FCAA077.

Assaf, Y., Blumenfeld-Katzir, T., Yovel, Y., Basser, P.J., 2008. AxCaliber: a method for measuring axon diameter distribution from diffusion MRI. Magn. Reson. Med. 59, 1347–1354. https://doi.org/10.1002/MRM.21577.

Azzarito, M., Kyathanahally, S.P., Balbastre, Y., Seif, M., Blaiotta, C., Callaghan, M.F., Ashburner, J., Freund, P., 2021. Simultaneous voxel-wise analysis of brain and spinal cord morphometry and microstructure within the <scp>SPM</scp> framework. Hum. Brain Mapp. 42, 220–232. https://doi.org/10.1002/hbm.25218.

Bagnato, F., Hametner, S., Yao, B., Van Gelderen, P., Merkle, H., Cantor, F.K., Lassmann, H., Duyn, J.H., 2011. Tracking iron in multiple sclerosis: a combined imaging and histopathological study at 7 Tesla. Brain 134, 3602–3615. https://doi.org/10.1093/BRAIN/AWR278.

Bakshi, R., Thompson, A.J., Rocca, M.A., Pelletier, D., Dousset, V., Barkhof, F., Inglese, M., Guttmann, C.R., Horsfield, M.A., Filippi, M., 2008. MRI in multiple sclerosis: current status and future prospects. Lancet Neurol. 7, 615–625. https://doi.org/10.1016/S1474-4422(08)70137-6.

Barazany, D., Basser, P.J., Assaf, Y., 2009. In vivo measurement of axon diameter distribution in the corpus callosum of rat brain. Brain 132, 1210–1220. https://doi.org/10.1093/BRAIN/AWP042.

Barry, R.L., Smith, S.A., Dula, A.N., Gore, J.C., 2014. Resting state functional connectivity in the human spinal cord. Elife 3, 1–15. https://doi.org/10.7554/eLife.02812.

Barry, R.L., Rogers, B.P., Conrad, B.N., Smith, S.A., Gore, J.C., 2016. Reproducibility of resting state spinal cord networks in healthy volunteers at 7 Tesla. Neuroimage 133, 31–40. https://doi.org/10.1016/j.neuroimage.2016.02.058.

Barry, R.L., Conrad, B.N., Smith, S.A., Gore, J.C., 2018a. A practical protocol for measurements of spinal cord functional connectivity. Sci. Rep. 8, 1–10. https://doi.org/10.1038/s41598-018-34841-6.

Barry, R.L., Vannesjo, S.J., By, S., Gore, J.C., Smith, S.A., 2018b. Spinal cord MRI at 7T. Neuroimage 168, 437–451. https://doi.org/10.1016/j.neuroimage.2017.07.003.

Basha, M.A.A., Bessar, M.A., Ahmed, A.F., Elfiki, I.M., Elkhatib, T.H.M., Mohamed, A.M. E., 2018. Does MR spectroscopy of normal-appearing cervical spinal cord in patients with multiple sclerosis have diagnostic value in assessing disease progression? A prospective comparative analysis. Clin. Radiol. 73, 835.e1–835.e9. https://doi.org/10.1016/J.CRAD.2018.04.018.

Basser, P.J., Pajevic, S., Pierpaoli, C., Duda, J., Aldroubi, A., 2000. In vivo fiber tractography using DT-MRI data. Magn. Reson. Med. 44, 625–632. https://doi.org/10.1002/1522-2594(200010)44:4<625::AID-MRM17>3.0.CO;2-O.

Battiston, M., Grussu, F., Ianus, A., Schneider, T., Prados, F., Fairney, J., Ourselin, S., Alexander, D.C., Cercignani, M., Gandini Wheeler-Kingshott, C.A.M., Samson, R.S., 2018. An optimized framework for quantitative magnetization transfer imaging of the cervical spinal cord in vivo. Magn. Reson. Med. 79, 2576–2588. https://doi.org/10.1002/mrm.26909.

Behrens, T.E.J., Woolrich, M.W., Jenkinson, M., Johansen-Berg, H., Nunes, R.G., Clare, S., Matthews, P.M., Brady, J.M., Smith, S.M., 2003. Characterization and propagation of uncertainty in diffusion-weighted MR imaging. Magn. Reson. Med. 50, 1077–1088. https://doi.org/10.1002/MRM.10609.

Bellenberg, B., Schneider, R., Weiler, F., Suchan, B., Haghikia, A., Hoffjan, S., Gold, R., Köster, O., Lukas, C., 2015. Cervical cord area is associated with infratentorial grey and white matter volume predominantly in relapsing-remitting multiple sclerosis: A study using semi-automated cord volumetry and voxel-based morphometry. Mult. Scler. Relat. Disord. 4, 264–272. https://doi.org/10.1016/j.msard.2015.04.003.

Bischof, A., Papinutto, N., Keshavan, A., Rajesh, A., Kirkish, G., Zhang, X., Mallott, J.M., Asteggiano, C., Sacco, S., Gundel, T.J., Zhao, C., Stern, W.A., Caverzasi, E., Zhou, Y., Gomez, R., Ragan, N.R., Santaniello, A., Zhu, A.H., Juwono, J., Bevan, C.J., Bove, R. M., Crabtree, E., Gelfand, J.M., Goodin, D.S., Graves, J.S., Green, A.J., Oksenberg, J. R., Waubant, E., Wilson, M.R., Zamvil, S.S., Cree, B.A.C., Hauser, S.L., Henry, R.G., 2022. Spinal cord atrophy predicts progressive disease in relapsing multiple sclerosis. Ann. Neurol. 91 (2), 268–281.

Blaiotta, C., Freund, P., Cardoso, M.J., Ashburner, J., 2018. Generative diffeomorphic modelling of large MRI data sets for probabilistic template construction. Neuroimage 166, 117–134. https://doi.org/10.1016/J.NEUROIMAGE.2017.10.060.

Bonacchi, R., Pagani, E., Meani, A., Cacciaguerra, L., Preziosa, P., de Meo, E., Filippi, M., Rocca, M.A., 2020. Clinical relevance of multiparametric MRI assessment of cervical cord damage in multiple sclerosis. Radiology 296, 605–615. https://doi.org/10.1148/RADIOL.2020200430.

Boonsuth, R., Samson, R.S., Tur, C., Battiston, M., Grussu, F., Schneider, T., Yoneyama, M., Prados, F., Ttofalla, A., Collorone, S., Cortese, R., Ciccarelli, O., Gandini Wheeler-Kingshott, C.A.M.M., Yiannakas, M.C., 2021. Assessing lumbar plexus and sciatic nerve damage in relapsing-remitting multiple sclerosis using magnetisation transfer ratio. Front. Neurol. 12, 2091. https://doi.org/10.3389/fneur.2021.763143.

Browne, C., Salmon, N., Kehoe, M., 2015. Bladder dysfunction and quality of life for people with multiple sclerosis. Disabil. Rehabil. 37, 2350–2358. https://doi.org/10.3109/09638288.2015.1027007.

By, S., Smith, A.K., Dethrage, L.M., Lyttle, B.D., Landman, B.A., Creasy, J.L., Pawate, S., Smith, S.A., 2016. Quantifying the impact of underlying measurement error on cervical spinal cord diffusion tensor imaging at 3T. J. Magn. Reson. Imaging 44, 1608–1618. https://doi.org/10.1002/jmri.25308.

By, S., Xu, J., Box, B.A., Bagnato, F.R., Smith, S.A., 2017. Application and evaluation of NODDI in the cervical spinal cord of multiple sclerosis patients. NeuroImage Clin. 15, 333–342. https://doi.org/10.1016/J.NICL.2017.05.010.

By, S., Barry, R.L., Smith, A.K., Lyttle, B.D., Box, B.A., Bagnato, F.R., Pawate, S., Smith, S. A., 2018a. Amide proton transfer CEST of the cervical spinal cord in multiple sclerosis patients at 3T. Magn. Reson. Med. 79, 806–814. https://doi.org/10.1002/mrm.26736.

By, S., Xu, J., Box, B.A., Bagnato, F.R., Smith, S.A., 2018b. Multi-compartmental diffusion characterization of the human cervical spinal cord in vivo using the spherical mean technique. NMR Biomed. 31 https://doi.org/10.1002/nbm.3894.

Catani, M., Howard, R.J., Pajevic, S., Jones, D.K., 2002. Virtual in vivo interactive dissection of white matter fasciculi in the human brain. Neuroimage 17, 77–94. https://doi.org/10.1006/NIMG.2002.1136.

Cercignani, M., Gandini Wheeler-Kingshott, C., 2019. From micro- to macro-structures in multiple sclerosis: what is the added value of diffusion imaging. NMR Biomed. 32 https://doi.org/10.1002/nbm.3888.

Chen, J.T., Collins, D.L., Atkins, H.L., Freedman, M.S., Arnold, D.L., Antel, J.P., Bar-Or, A., Bence-Bruckler, I., Duquette, P., Huebsch, L., Laneuville, P., Lapierre, Y., Messner, H., Pierre Sekaly, R., O'Connor, P., Halpenny, M., 2008. Magnetization transfer ratio evolution with demyelination and remyelination in multiple sclerosis lesions. Ann. Neurol. 63, 254–262. https://doi.org/10.1002/ANA.21302.

Chen, Y., Haacke, E.M., Bernitsas, E., 2020. Imaging of the spinal cord in multiple sclerosis: Past, present, future. Brain Sci. 10, 1–19. https://doi.org/10.3390/brainsci10110857.

Christiaens, D., Cordero-Grande, L., Pietsch, M., Hutter, J., Price, A.N., Hughes, E.J., Vecchiato, K., Deprez, M., Edwards, A.D., Hajnal, J.V., Tournier, J.D., 2021. Scattered slice SHARD reconstruction for motion correction in multi-shell diffusion MRI. Neuroimage 225, 117437. https://doi.org/10.1016/J.NEUROIMAGE.2020.117437.

Clarke, M.A., Pareto, D., Pessini-Ferreira, L., Arrambide, G., Alberich, M., Crescenzo, F., Cappelle, S., Tintoré, M., Sastre-Garriga, J., Auger, C., Montalban, X., Evangelou, N., Rovira, À., 2020. Value of 3T susceptibility-weighted imaging in the diagnosis of multiple sclerosis. Am. J. Neuroradiol. 41, 1001–1008. https://doi.org/10.3174/AJNR.A6547.

Cohen, A.B., Neema, M., Arora, A., Dell'Oglio, E., Benedict, R.H.B., Tauhid, S., Goldberg-Zimring, D., Chavarro-Nieto, C., Ceccarelli, A., Klein, J.P., Stankiewicz, J.M., Houtchens, M.K., Buckle, G.J., Alsop, D.C., Guttmann, C.R.G., Bakshi, R., 2012a. The relationships among MRI-defined spinal cord involvement, brain involvement, and disability in multiple sclerosis. J. Neuroimaging 22, 122–128. https://doi.org/10.1111/J.1552-6569.2011.00589.X.

Cohen, J., Reingold, S.C., Polman, C.H., Wolinsky, J.S., 2012b. Disability outcome measures in multiple sclerosis clinical trials: Current status and future prospects. Lancet Neurol. 11, 467–476. https://doi.org/10.1016/S1474-4422(12)70059-5.

Cohen-Adad, J., 2018. Microstructural imaging in the spinal cord and validation strategies. Neuroimage 182, 169–183. https://doi.org/10.1016/j.neuroimage.2018.04.009.

Cohen-Adad, J., 2021. High-Resolution DWI in Brain and Spinal Cord with syngo RESOLVE. MAGNETOM Flash 2, 16–23.

Cohen-Adad, J., Gauthier, C.J., Brooks, J.C.W., Slessarev, M., Han, J., Fisher, J.A., Rossignol, S., Hoge, R.D., 2010. BOLD signal responses to controlled hypercapnia in human spinal cord. Neuroimage 50, 1074–1084. https://doi.org/10.1016/J.NEUROIMAGE.2009.12.122.

Cohen-Adad, J., Alonso-Ortiz, E., Abramovic, M., Arneitz, C., Atcheson, N., Barlow, L., Barry, R.L., Barth, M., Battiston, M., Büchel, C., Budde, M., Callot, V., Combes, A.J. E., De Leener, B., Descoteaux, M., de Sousa, P.L., Dostál, M., Doyon, J., Dvorak, A., Eippert, F., Epperson, K.S.K.R., Epperson, K.S.K.R., Freund, P., Finsterbusch, J., Foias, A., Fratini, M., Fukunaga, I., Gandini Wheeler-Kingshott, C.A.M., Germani, G., Gilbert, G., Giove, F., Gros, C., Grussu, F., Hagiwara, A., Henry, P.G., Horák, T., Hori, M., Joers, J., Kamiya, K., Karbasforoushan, H., Keřkovský, M., Khatibi, A., Kim, J.W., Kinany, N., Kitzler, H.H., Kolind, S., Kong, Y., Kudlička, P., Kuntke, P., Kurniawan, N.D., Kusmia, S., Labounek, R., Laganà, M.M., Laule, C., Law, C.S., Lenglet, C., Leutritz, T., Liu, Y., Llufriu, S., Mackey, S., Martinez-Heras, E., Mattera, L., Nestrasil, I., O'Grady, K.P., Papinutto, N., Papp, D., Pareto, D., Parrish, T.B., Pichiecchio, A., Prados, F., Rovira, À., Ruitenberg, M.J., Samson, R.S., Savini, G., Seif, M., Seifert, A.C., Smith, A.K., Smith, S.A., Smith, Z.A., Solana, E., Suzuki, Y., Tackley, G., Tinnermann, A., Valošek, J., Van De Ville, D., Yiannakas, M. C., Weber, K.A., Weiskopf, N., Wise, R.G., Wyss, P.O., Xu, J., 2021a. Open-access quantitative MRI data of the spinal cord and reproducibility across participants, sites and manufacturers. Sci. Data 8, 219. https://doi.org/10.1038/s41597-021-00941-8.

Cohen-Adad, J., Alonso-Ortiz, E., Abramovic, M., Arneitz, C., Atcheson, N., Barlow, L., Barry, R.L., Barth, M., Battiston, M., Büchel, C., Budde, M., Callot, V., Combes, A.J. E., De Leener, B., Descoteaux, M., de Sousa, P.L., Dostál, M., Doyon, J., Dvorak, A., Eippert, F., Epperson, K.R., Epperson, K.S., Freund, P., Finsterbusch, J., Foias, A., Fratini, M., Fukunaga, I., Wheeler-Kingshott, C.A.M.G., Germani, G., Gilbert, G., Giove, F., Gros, C., Grussu, F., Hagiwara, A., Henry, P.-G., Horák, T., Hori, M., Joers, J., Kamiya, K., Karbasforoushan, H., Keřkovský, M., Khatibi, A., Kim, J.-W., Kinany, N., Kitzler, H., Kolind, S., Kong, Y., Kudlička, P., Kuntke, P., Kurniawan, N. D., Kusmia, S., Labounek, R., Laganà, M.M., Laule, C., Law, C.S., Lenglet, C., Leutritz, T., Liu, Y., Llufriu, S., Mackey, S., Martinez-Heras, E., Mattera, L., Nestrasil, I., O'Grady, K.P., Papinutto, N., Papp, D., Pareto, D., Parrish, T.B., Pichiecchio, A., Prados, F., Rovira, À., Ruitenberg, M.J., Samson, R.S., Savini, G., Seif, M., Seifert, A.C., Smith, A.K., Smith, S.A., Smith, Z.A., Solana, E., Suzuki, Y., Tackley, G., Tinnermann, A., Valošek, J., Van De Ville, D., Yiannakas, M.C., Weber, K.A., Weiskopf, N., Wise, R.G., Wyss, P.O., Xu, J., 2021b. Generic acquisition protocol for quantitative MRI of the spinal cord. Nat. Protoc. 16 (10), 4611–4632.

Cohen-Adad, J., Alonso-Ortiz, E., Alley, S., Lagana, M.M., Baglio, F., Vannesjo, S.J., Karbasforoushan, H., Seif, M., Seifert, A.C., Xu, J., Kim, J., Labounek, R., Vojtíšek, L., Dostál, M., Valošek, J., Samson, R.S., Grussu, F., Battiston, M., Gandini Wheeler-Kingshott, C.A.M., Yiannakas, M.C., Gilbert, G., Schneider, T., Johnson, B., Prados, F., 2022. Comparison of multicenter <scp>MRI</scp> protocols for visualizing the spinal cord gray matter. Magn. Reson. Med. https://doi.org/10.1002/MRM.29249.

Collorone, S., Cawley, N., Grussu, F., Prados, F., Tona, F., Calvi, A., Kanber, B., Schneider, T., Kipp, L., Zhang, H., Alexander, D.C., Thompson, A.J., Toosy, A., Wheeler-Kingshott, C.A.G., Ciccarelli, O., 2020. Reduced neurite density in the brain and cervical spinal cord in relapsing–remitting multiple sclerosis: A NODDI study. Mult. Scler. J. 26, 1647–1657. https://doi.org/10.1177/1352458519885107.

Combès, B., Monteau, L., Bannier, E., Callot, V., Labauge, P., Ayrignac, X., Carra Dallière, C., Pelletier, J., Maarouf, A., de Seze, J., Collongues, N., Barillot, C., Edan, G., Ferré, J.C., Kerbrat, A., 2019. Measurement of magnetization transfer ratio (MTR) from cervical spinal cord: Multicenter reproducibility and variability. J. Magn. Reson. Imaging 49 (6), 1777–1785.

Combes, A.J.E., O'Grady, K.P., Rogers, B.P., Schilling, K.G., Lawless, R.D., Visagie, M., Houston, D., Prock, L., Malone, S., Satish, S., Witt, A.A., McKnight, C.D., Bagnato, F., Gore, J.C., Smith, S.A., 2022. Functional connectivity in the dorsal network of the cervical spinal cord is correlated with diffusion tensor imaging indices in relapsing-remitting multiple sclerosis. NeuroImage Clin. 35, 103127 https://doi.org/10.1016/j.nicl.2022.103127.

Conrad, B.N., Barry, R.L., Rogers, B.P., Maki, S., Mishra, A., Thukral, S., Sriram, S., Bhatia, A., Pawate, S., Gore, J.C., Smith, S.A., 2018. Multiple sclerosis lesions affect intrinsic functional connectivity of the spinal cord. Brain 141, 1650–1664. https://doi.org/10.1093/brain/awy083.

Cordero-Grande, L., Christiaens, D., Hutter, J., Price, A.N., Hajnal, J.V., 2019. Complex diffusion-weighted image estimation via matrix recovery under general noise models. Neuroimage 200, 391–404. https://doi.org/10.1016/J.NEUROIMAGE.2019.06.039.

Daams, M., Weiler, F., Steenwijk, M.D., Hahn, H.K., Geurts, J.J.G., Vrenken, H., Van Schijndel, R.A., Balk, L.J., Tewarie, P.K., Tillema, J.M., Killestein, J., Uitdehaag, B.M. J., Barkhof, F., 2014. Mean upper cervical cord area (MUCCA) measurement in long-standing multiple sclerosis: Relation to brain findings and clinical disability. Mult. Scler. J. 20, 1860–1865. https://doi.org/10.1177/1352458514533399.

Dal-Bianco, A., Grabner, G., Kronnerwetter, C., Weber, M., Höftberger, R., Berger, T., Auff, E., Leutmezer, F., Trattnig, S., Lassmann, H., Bagnato, F., Hametner, S., 2017. Slow expansion of multiple sclerosis iron rim lesions: pathology and 7 T magnetic resonance imaging. Acta Neuropathol. 133, 25–42. https://doi.org/10.1007/S00401-016-1636-Z.

Dawson, J.W., 1916. XVIII.—The histology of disseminated sclerosis. Trans. R. Soc. Edinburgh 50 (3), 517–740.

De Leener, B., Fonov, V.S., Collins, D.L., Callot, V., Stikov, N., Cohen-Adad, J., 2018. PAM50: Unbiased multimodal template of the brainstem and spinal cord aligned with the ICBM152 space, in: NeuroImage. Honolulu, Hawaii, pp. 170–179. doi: 10.1016/j.neuroimage.2017.10.041.

De Leener, B., Mangeat, G., Dupont, S., Martin, A.R., Callot, V., Stikov, N., Fehlings, M. G., Cohen-Adad, J., 2017. Topologically preserving straightening of spinal cord MRI. J. Magn. Reson. Imaging 46 (4), 1209–1219.

De Stefano, N., Battaglini, M., Pareto, D., Cortese, R., Zhang, J., Oesingmann, N., Prados, F., Rocca, M.A., Valsasina, P., Vrenken, H., Gandini Wheeler-Kingshott, C.A. M., Filippi, M., Barkhof, F., Rovira, À., 2022. MAGNIMS recommendations for harmonization of MRI data in MS multicenter studies. NeuroImage Clin. 34, 102972 https://doi.org/10.1016/J.NICL.2022.102972.

Demortière, S., Lehmann, P., Pelletier, J., Audoin, B., Callot, V., 2020. Improved Cervical Cord Lesion Detection with 3D-MP2RAGE Sequence in Patients with Multiple Sclerosis. Am. J. Neuroradiol. 41, 1131–1134. https://doi.org/10.3174/ajnr.A6567.

Dula, A.N., Pawate, S., Dethrage, L.M., Conrad, B.N., Dewey, B.E., Barry, R.L., Smith, S. A., 2016a. Chemical exchange saturation transfer of the cervical spinal cord at 7 T. NMR Biomed. 29, 1249–1257. https://doi.org/10.1002/nbm.3581.

Dula, A.N., Pawate, S., Dortch, R.D., Barry, R.L., George-Durrett, K.M., Lyttle, B.D., Dethrage, L.M., Gore, J.C., Smith, S.A., 2016b. Magnetic resonance imaging of the cervical spinal cord in multiple sclerosis at 7T. Mult. Scler. J. 22, 320–328. https://doi.org/10.1177/1352458515591070.

Duval, T., Lévy, S., Stikov, N., Cohen-Adad, J., Stikov, N., Campbell, J., Mezer, A., Witzel, T., Keil, B., Smith, V., Wald, L.L.L., Klawiter, E., Lévy, S., Cohen-Adad, J., 2017. g-Ratio weighted imaging of the human spinal cord in vivo. Neuroimage 145, 11–23. https://doi.org/10.1016/j.neuroimage.2016.09.018.

Duval, T., Smith, V., Stikov, N., Klawiter, E.C., Cohen-Adad, J., 2018. Scan–rescan of axcaliber, macromolecular tissue volume, and g-ratio in the spinal cord. Magn. Reson. Med. 79, 2759–2765. https://doi.org/10.1002/mrm.26945.

Dvorak, A.V., Ljungberg, E., Vavasour, I.M., Liu, H., Johnson, P., Rauscher, A., Kramer, J. L.K., Tam, R., Li, D.K.B., Laule, C., Barlow, L., Briemberg, H., MacKay, A.L., Traboulsee, A., Kozlowski, P., Cashman, N., Kolind, S.H., 2019. Rapid myelin water imaging for the assessment of cervical spinal cord myelin damage. NeuroImage Clin. 23, 101896 https://doi.org/10.1016/J.NICL.2019.101896.

Dvorak, A.V., Ljungberg, E., Vavasour, I.M., Lee, L.E., Abel, S., Li, D.K.B., Traboulsee, A., MacKay, A.L., Kolind, S.H., 2021. Comparison of multi echo T2 relaxation and steady state approaches for myelin imaging in the central nervous system. Sci. Rep. 11 (1).

Eden, D., Gros, C., Badji, A., Dupont, S.M., De Leener, B., Maranzano, J., Zhuoquiong, R., Liu, Y., Granberg, T., Ouellette, R., Stawiarz, L., Hillert, J., Talbott, J., Bannier, E., Kerbrat, A., Edan, G., Labauge, P., Callot, V., Pelletier, J., Audoin, B., Rasoanandrianina, H., Brisset, J.-C.-C., Valsasina, P., Rocca, M.A., Filippi, M., Bakshi, R., Tauhid, S., Prados, F., Yiannakas, M., Kearney, H., Ciccarelli, O., Smith, S. A., Andrada Treaba, C., Mainero, C., Lefeuvre, J., Reich, D.S., Nair, G., Shepherd, T. M., Charlson, E., Tachibana, Y., Hori, M., Kamiya, K., Chougar, L., Narayanan, S., Cohen-Adad, J., 2019. Spatial distribution of multiple sclerosis lesions in the cervical spinal cord. Brain 142, 633–646. https://doi.org/10.1093/brain/awy352.

Edwards, E.M., Wu, W., Fritz, N.E., 2022. Using myelin water imaging to link underlying pathology to clinical function in multiple sclerosis: A scoping review. Mult. Scler. Relat. Disord. 59, 103646 https://doi.org/10.1016/j.msard.2022.103646.

Eippert, F., Kong, Y., Jenkinson, M., Tracey, I., Brooks, J.C.W., 2017. Denoising spinal cord fMRI data: Approaches to acquisition and analysis. Neuroimage 154, 255–266. https://doi.org/10.1016/j.neuroimage.2016.09.065.

Fadnavis, S., Batson, J., Garyfallidis, E., 2020. Patch2Self: Denoising Diffusion MRI with Self-Supervised Learning. Adv. Neural Inf. Process. Syst. 2020-December. doi: 10.48550/arxiv.2011.01355.

Fan, Q., Nummenmaa, A., Wichtmann, B., Witzel, T., Mekkaoui, C., Schneider, W., Wald, L.L., Huang, S.Y., 2018. Validation of diffusion MRI estimates of compartment size and volume fraction in a biomimetic brain phantom using a human MRI scanner with 300 mT/m maximum gradient strength. Neuroimage 182, 469–478. https://doi.org/10.1016/J.NEUROIMAGE.2018.01.004.

Fechner, A., Savatovsky, J., El Methni, J., Sadik, J.C., Gout, O., Deschamps, R., Gueguen, A., Lecler, A., 2019. A 3T phase-sensitive inversion recovery MRI sequence improves detection of cervical spinal cord lesions and shows active lesions in patients with multiple sclerosis. Am. J. Neuroradiol. 40, 370–375. https://doi.org/10.3174/ajnr.A5941.

Figley, C.R., Yau, D., Stroman, P.W., 2008. Attenuation of lower-thoracic, lumbar, and sacral spinal cord motion: Implications for imaging human spinal cord structure and function. Am. J. Neuroradiol. 29, 1450–1454. https://doi.org/10.3174/ajnr.A1154.

Filippi, M., Rocca, M.A., Falini, A., Caputo, D., Ghezzi, A., Colombo, B., Scotti, G., Comi, G., 2002. Correlations between structural CNS damage and functional MRI changes in primary progressive MS. Neuroimage 15, 537–546. https://doi.org/10.1006/NIMG.2001.1023.

Filippi, M., Preziosa, P., Banwell, B.L., Barkhof, F., Ciccarelli, O., De Stefano, N., Geurts, J.J.G., Paul, F., Reich, D.S., Toosy, A.T., Traboulsee, A., Wattjes, M.P., Yousry, T.A., Gass, A., Lubetzki, C., Weinshenker, B.G., Rocca, M.A., 2019. Assessment of lesions on magnetic resonance imaging in multiple sclerosis: practical guidelines. Brain 142, 1858–1875. https://doi.org/10.1093/BRAIN/AWZ144.

Finsterbusch, J., Sprenger, C., Büchel, C., 2013. Combined T2*-weighted measurements of the human brain and cervical spinal cord with a dynamic shim update. Neuroimage 79, 153–161. https://doi.org/10.1016/J.NEUROIMAGE.2013.04.021.

Forodighasemabadi, A., Rasoanandrianina, H., El Mendili, M.M., Guye, M., Callot, V., 2021. An optimized MP2RAGE sequence for studying both brain and cervical spinal cord in a single acquisition at 3T. Magn. Reson. Imaging 84, 18–26. https://doi.org/10.1016/J.MRI.2021.08.011.

Freund, P., Papinutto, N., Bischof, A., Azzarito, M., Kirkish, G., Ashburner, J., Thompson, A., Hauser, S.L., Henry, R.G., 2022. Simultaneous assessment of regional distributions of atrophy across the neuraxis in MS patients. NeuroImage Clin. 34, 102985 https://doi.org/10.1016/j.nicl.2022.102985.

Furby, J., Hayton, T., Anderson, V., Altmann, D., Brenner, R., Chataway, J., Hughes, R.A. C., Smith, K.J., Miller, D.H., Kapoor, R., 2008. Magnetic resonance imaging measures of brain and spinal cord atrophy correlate with clinical impairment in secondary progressive multiple sclerosis. Mult. Scler. 14, 1068–1075. https://doi.org/10.1177/1352458508093617.

Gass, A., Rocca, M.A., Agosta, F., Ciccarelli, O., Chard, D., Valsasina, P., Brooks, J.C.W., Bischof, A., Eisele, P., Kappos, L., Barkhof, F., Filippi, M., 2015. MRI monitoring of pathological changes in the spinal cord in patients with multiple sclerosis. Lancet Neurol. 14, 443–454. https://doi.org/10.1016/S1474-4422(14)70294-7.

Gilmore, C.P., Bö, L., Owens, T., Lowe, J., Esiri, M.M., Evangelou, N., 2006. Spinal cord gray matter demyelination in multiple sclerosis - A novel pattern of residual plaque morphology. Brain Pathol. 16, 202–208. https://doi.org/10.1111/J.1750-3639.2006.00018.X.

Gilmore, C.P., Donaldson, I., Bö, L., Owens, T., Lowe, J., Evangelou, N., 2009. Regional variations in the extent and pattern of grey matter demyelination in multiple sclerosis: a comparison between the cerebral cortex, cerebellar cortex, deep grey matter nuclei and the spinal cord. J. Neurol. Neurosurg. Psychiatry 80, 182–187. https://doi.org/10.1136/JNNP.2008.148767.

Girard, O.M., Callot, V., Prevost, V.H., Robert, B., Taso, M., Ribeiro, G., Varma, G., Rangwala, N., Alsop, D.C., Duhamel, G., 2017. Magnetization transfer from inhomogeneously broadened lines (ihMT): Improved imaging strategy for spinal cord applications. Magn. Reson. Med. 77, 581–591. https://doi.org/10.1002/MRM.26134.

Granziera, C., Wuerfel, J., Barkhof, F., Calabrese, M., De Stefano, N., Enzinger, C., Evangelou, N., Filippi, M., Geurts, J.J.G., Reich, D.S., Rocca, M.A., Ropele, S., Rovira, À., Sati, P., Toosy, A.T., Vrenken, H., Gandini Wheeler-Kingshott, C.A.M., Kappos, L., Barkhof, F., de Stefano, N., Sastre-Garriga, J., Ciccarelli, O., Enzinger, C., Filippi, M., Gasperini, C., Kappos, L., Palace, J., Vrenken, H., Rovira, À., Rocca, M.A., Yousry, T., 2021. Quantitative magnetic resonance imaging towards clinical application in multiple sclerosis. Brain 144 (5), 1296–1311.

Gros, C., De Leener, B., Badji, A., Maranzano, J., Eden, D., Dupont, S.M., Talbott, J., Zhuoquiong, R., Liu, Y., Granberg, T., Ouellette, R., Tachibana, Y., Hori, M., Kamiya, K., Chougar, L., Stawiarz, L., Hillert, J., Bannier, E., Kerbrat, A., Edan, G., Labauge, P., Callot, V., Pelletier, J., Audoin, B., Rasoanandrianina, H., Brisset, J.C., Valsasina, P., Rocca, M.A., Filippi, M., Bakshi, R., Tauhid, S., Prados, F., Yiannakas, M., Kearney, H., Ciccarelli, O., Smith, S., Treaba, C.A., Mainero, C., Lefeuvre, J., Reich, D.S., Nair, G., Auclair, V., McLaren, D.G., Martin, A.R., Fehlings, M.G., Vahdat, S., Khatibi, A., Doyon, J., Shepherd, T., Charlson, E., Narayanan, S., Cohen-Adad, J., 2019. Automatic segmentation of the spinal cord and intramedullary multiple sclerosis lesions with convolutional neural networks. Neuroimage 184, 901–915. https://doi.org/10.1016/J.NEUROIMAGE.2018.09.081.

Grussu, F., Schneider, T., Zhang, H., Alexander, D.C., Wheeler-Kingshott, C.A.M., 2015. Neurite orientation dispersion and density imaging of the healthy cervical spinal cord in vivo. Neuroimage 111, 590–601. https://doi.org/10.1016/j.neuroimage.2015.01.045.

Grussu, F., Schneider, T., Tur, C., Yates, R.L., Tachrount, M., Ianuş, A., Yiannakas, M.C., Newcombe, J., Zhang, H., Alexander, D.C., DeLuca, G.C., Gandini Wheeler-Kingshott, C.A.M., 2017. Neurite dispersion: a new marker of multiple sclerosis spinal cord pathology? 4, 663–679. doi: 10.1002/ACN3.445.

Grussu, F., Ianuş, A., Tur, C., Prados, F., Schneider, T., Kaden, E., Ourselin, S., Drobnjak, I., Zhang, H., Alexander, D.C., Gandini Wheeler-Kingshott, C.A.M., 2019. Relevance of time-dependence for clinically viable diffusion imaging of the spinal cord. Magn. Reson. Med. 81, 1247–1264. https://doi.org/10.1002/MRM.27463.

Grussu, F., Battiston, M., Veraart, J., Schneider, T., Cohen-Adad, J., Shepherd, T.M., Alexander, D.C., Fieremans, E., Novikov, D.S., Gandini Wheeler-Kingshott, C.A.M., 2020. Multi-parametric quantitative in vivo spinal cord MRI with unified signal readout and image denoising. Neuroimage 217, 116884. https://doi.org/10.1016/j.neuroimage.2020.116884.

Horsfield, M.A., Sala, S., Neema, M., Absinta, M., Bakshi, A., Sormani, M.P., Rocca, M.A., Bakshi, R., Filippi, M., 2010. Rapid semi-automatic segmentation of the spinal cord from magnetic resonance images: application in multiple sclerosis. Neuroimage 50, 446–455. https://doi.org/10.1016/j.neuroimage.2009.12.121.

Hu, Y., Jin, R., Li, G., Luk, K.D.K.D., Wu, E.X., 2018. Robust spinal cord resting-state fMRI using independent component analysis-based nuisance regression noise reduction. J. Magn. Reson. Imaging 48, 1421–1431. https://doi.org/10.1002/jmri.26048.

Hua, L.H., Donlon, S.L., Sobhanian, M.J., Portner, S.M., Okuda, D.T., 2015. Thoracic spinal cord lesions are influenced by the degree of cervical spine involvement in multiple sclerosis. Spinal Cord 53 (7), 520–525.

Huhn, K., Engelhorn, T., Linker, R.A., Nagel, A.M., 2019. Potential of sodium MRI as a biomarker for neurodegeneration and neuroinflammation in multiple sclerosis. Front. Neurol. 10, 84. https://doi.org/10.3389/FNEUR.2019.00084/BIBTEX.

Ineichen, B.V., Beck, E.S., Piccirelli, M., Reich, D.S., 2021. New prospects for ultra-high-field magnetic resonance imaging in multiple sclerosis. Invest. Radiol. Publish Ah 56 (11), 773–784.

Ingle, G.T., Stevenson, V.L., Miller, D.H., Thompson, A.J., 2003. Primary progressive multiple sclerosis: a 5-year clinical and MR study. Brain 126, 2528–2536. https://doi.org/10.1093/BRAIN/AWG261.

Islam, H., Law, C.S.W., Weber, K.A., Mackey, S.C., Glover, G.H., 2019. Dynamic per slice shimming for simultaneous brain and spinal cord fMRI. Magn. Reson. Med. 81, 825–838. https://doi.org/10.1002/mrm.27388.

Jelescu, I.O., Veraart, J., Adisetiyo, V., Milla, S.S., Novikov, D.S., Fieremans, E., 2015. One diffusion acquisition and different white matter models: how does microstructure change in human early development based on WMTI and NODDI? Neuroimage 107, 242–256. https://doi.org/10.1016/J.NEUROIMAGE.2014.12.009.

Jelescu, I.O., Veraart, J., Fieremans, E., Novikov, D.S., 2016. Degeneracy in model parameter estimation for multi-compartmental diffusion in neuronal tissue. NMR Biomed. 29, 33–47. https://doi.org/10.1002/NBM.3450.

Jelescu, I.O., Palombo, M., Bagnato, F., Schilling, K.G., 2020. Challenges for biophysical modeling of microstructure. J. Neurosci. Methods 344, 108861.

Jende, J.M.E., Hauck, G.H., Diem, R., Weiler, M., Heiland, S., Wildemann, B., Korporal-Kuhnke, M., Wick, W., Hayes, J.M., Pfaff, J., Pham, M., Bendszus, M., Kollmer, J., 2017. Peripheral nerve involvement in multiple sclerosis: demonstration by magnetic resonance neurography. Ann. Neurol. 82, 676–685. https://doi.org/10.1002/ANA.25068.

Jensen-Kondering, U., Larsen, N., Huhndorf, M., Jansen, O., Lüddecke, R., Stürner, K., Salehi Ravesh, M., 2022. Central vein sign in patients with inflammatory lesion of the upper cervical spinal cord on susceptibility weighted imaging at 3 tesla. Preliminary results. Magn. Reson. Imaging 93, 11–14. https://doi.org/10.1016/j.mri.2022.07.013.

Jeong, H.K., Gore, J.C., Anderson, A.W., 2013. High-resolution human diffusion tensor imaging using 2-D navigated multishot SENSE EPI at 7 T. Magn. Reson. Med. 69, 793–802. https://doi.org/10.1002/MRM.24320.

Jones, D.K., Cercignani, M., 2010. Twenty-five pitfalls in the analysis of diffusion MRI data. NMR Biomed. 23, 803–820. https://doi.org/10.1002/nbm.1543.

Jones, D.K., Horsfield, M.A., Simmons, A., 1999. Optimal strategies for measuring diffusion in anisotropic systems by magnetic resonance imaging. Magn. Reson. Med. 42, 515–525. https://doi.org/10.1002/(SICI)1522-2594(199909)42:3<515::AID-MRM14>3.0.CO;2-Q.

Kaden, E., Kelm, N.D., Carson, R.P., Does, M.D., Alexander, D.C., 2016. Multi-compartment microscopic diffusion imaging. Neuroimage 139, 346–359. https://doi.org/10.1016/J.NEUROIMAGE.2016.06.002.

Karampinos, D.C., Van, A.T., Olivero, W.C., Georgiadis, J.G., Sutton, B.P., 2009. High-resolution diffusion tensor imaging of the human pons with a reduced field-of-view, multishot, variable-density, spiral acquisition at 3 T. Magn. Reson. Med. 62, 1007–1016. https://doi.org/10.1002/MRM.22105.

Kearney, H., Schneider, T., Yiannakas, M.C., Altmann, D.R., Wheeler-Kingshott, C.A.M., Ciccarelli, O., Miller, D.H., 2015. Spinal cord grey matter abnormalities are associated with secondary progression and Physical disability in multiple sclerosis. J. Neurol. Neurosurg. Psychiatry 86, 608–614. https://doi.org/10.1136/jnnp-2014-308241.

Kerbrat, A., Gros, C., Badji, A., Bannier, E., Galassi, F., Combès, B., Chouteau, R., Labauge, P., Ayrignac, X., Carra-Dalliere, C., Maranzano, J., Granberg, T., Ouellette, R., Stawiarz, L., Hillert, J., Talbott, J., Tachibana, Y., Hori, M., Kamiya, K., Chougar, L., Lefeuvre, J., Reich, D.S., Nair, G., Valsasina, P., Rocca, M.A., Filippi, M., Chu, R., Bakshi, R., Callot, V., Pelletier, J., Audoin, B., Maarouf, A., Collongues, N., de Seze, J., Edan, G., Cohen-Adad, J., 2020. Multiple sclerosis lesions in motor tracts from brain to cervical cord: Spatial distribution and correlation with disability. Brain 143, 2089–2105. https://doi.org/10.1093/brain/awaa162.

Kinany, N., Pirondini, E., Micera, S., Van De Ville, D., 2020. Dynamic Functional Connectivity of Resting-State Spinal Cord fMRI Reveals Fine-Grained Intrinsic Architecture. Neuron 108, 424–435.e4. https://doi.org/10.1016/j.neuron.2020.07.024.

Kinany, N., Pirondini, E., Mattera, L., Martuzzi, R., Micera, S., Van De Ville, D., 2022. Towards reliable spinal cord fMRI: assessment of common imaging protocols. Neuroimage 250, 118964. https://doi.org/10.1016/j.neuroimage.2022.118964.

Kisel, A.A., Naumova, A.V., Yarnykh, V.L., 2022. Macromolecular proton fraction as a myelin biomarker: principles, validation, and applications. Front. Neurosci. 16 https://doi.org/10.3389/fnins.2022.819912.

Kister, I., Bacon, T.E., Chamot, E., Salter, A.R., Cutter, G.R., Kalina, J.T., Herbert, J., 2013. Natural history of multiple sclerosis symptoms. Int. J. MS Care 15, 146–158. https://doi.org/10.7224/1537-2073.2012-053.

Klawiter, E.C., Schmidt, R.E., Trinkaus, K., Liang, H.F., Budde, M.D., Naismith, R.T., Song, S.K., Cross, A.H., Benzinger, T.L., 2011. Radial diffusivity predicts

demyelination in ex vivo multiple sclerosis spinal cords. Neuroimage 55, 1454–1460. https://doi.org/10.1016/j.neuroimage.2011.01.007.
Kleesiek, J., Urban, G., Hubert, A., Schwarz, D., Maier-Hein, K., Bendszus, M., Biller, A., 2016. Deep MRI brain extraction: a 3D convolutional neural network for skull stripping. Neuroimage 129, 460–469. https://doi.org/10.1016/J.NEUROIMAGE.2016.01.024.
Kogan, F., Singh, A., Debrosse, C., Haris, M., Cai, K., Nanga, R.P., Elliott, M., Hariharan, H., Reddy, R., 2013. Imaging of glutamate in the spinal cord using GluCEST. Neuroimage 77, 262–267. https://doi.org/10.1016/j.neuroimage.2013.03.072.
Kolesar, T.A., Fiest, K.M., Smith, S.D., Kornelsen, J., 2015. Assessing nociception by fmri of the human spinal cord: a systematic review. Magn. Reson. Insights 8s1, MRI.S23556.
Kolind, S., Seddigh, A., Combes, A., Russell-Schulz, B., Tam, R., Yogendrakumar, V., Deoni, S., Sibtain, N.A., Traboulsee, A., Williams, S.C.R., Barker, G.J., Brex, P.A., 2015. Brain and cord myelin water imaging: a progressive multiple sclerosis biomarker. NeuroImage Clin. 9, 574–580. https://doi.org/10.1016/j.nicl.2015.10.002.
Kong, Y., Eippert, F., Beckmann, C.F., Andersson, J., Finsterbusch, J., Büchel, C., Tracey, I., Brooks, J.C.W., 2014. Intrinsically organized resting state networks in the human spinal cord. Proc. Natl. Acad. Sci. U. S. A. 111, 18067–18072. https://doi.org/10.1073/pnas.1414293111.
Kontopodis, E.E., Papadaki, E., Trivizakis, E., Maris, T.G., Simos, P., Papadakis, G.Z., Tsatsakis, A., Spandidos, D.A., Karantanas, A., Marias, K., 2021. Emerging deep learning techniques using magnetic resonance imaging data applied in multiple sclerosis and clinical isolated syndrome patients (Review). Exp. Ther. Med. 22 https://doi.org/10.3892/ETM.2021.10583.
Kreiter, D.J., van den Hurk, J., Wiggins, C.J., Hupperts, R.M.M., Gerlach, O.H.H., 2022. Ultra-high field spinal cord MRI in multiple sclerosis: Where are we standing? A literature review. Mult. Scler. Relat. Disord. 57, 103436 https://doi.org/10.1016/j.msard.2021.103436.
Krieger, S., 2022. On cave paintings and shallow waters—the case for advancing spinal cord imaging in multiple sclerosis. JAMA Neurol. 79, 9–10. https://doi.org/10.1001/JAMANEUROL.2021.4245.
Krieger, S.C., Cook, K., de Nino, S., Fletcher, M., 2016. The topographical model of multiple sclerosis: a dynamic visualization of disease course. Neurol. Neuroimmunol. NeuroInflammation 3, e279. doi: 10.1212/NXI.0000000000000279.
Lakhani, D.A., Schilling, K.G., Xu, J., Bagnato, F., 2020. Advanced multicompartment diffusion MRI models and their application in multiple sclerosis. Am. J. Neuroradiol. 41, 751–757. https://doi.org/10.3174/AJNR.A6484.
Landman, B.A., Farrell, J.A.D., Jones, C.K., Smith, S.A., Prince, J.L., Mori, S., 2007. Effects of diffusion weighting schemes on the reproducibility of DTI-derived fractional anisotropy, mean diffusivity, and principal eigenvector measurements at 1.5T. Neuroimage 36, 1123–1138. https://doi.org/10.1016/J.NEUROIMAGE.2007.02.056.
Lapointe, E., Li, D.K.B., Traboulsee, A.L., Rauscher, A., 2018. What have we learned from perfusion MRI in multiple sclerosis? Am. J. Neuroradiol. 39, 994–1000. https://doi.org/10.3174/ajnr.A5504.
Laule, C., Moore, G.R.W., 2018. Myelin water imaging to detect demyelination and remyelination and its validation in pathology. Brain Pathol. 28 (5), 750–764.
Laule, C., Yung, A., Pavolva, V., Bohnet, B., Kozlowski, P., Hashimoto, S.A., Yip, S., Li, D.KB., Moore, GR.W., 2016. High-resolution myelin water imaging in post-mortem multiple sclerosis spinal cord: a case report. Mult Scler 22 (11), 1485–1489.
Lee, J.J., Hyun, J.W., Lee, J.J., Choi, E.J., Shin, H.G., Min, K., Nam, Y., Kim, H.J., Oh, S.H., 2020. So you want to image myelin using MRI: an overview and practical guide for myelin water imaging. J. Magn. Reson. Imaging 53, 1–14. https://doi.org/10.1002/jmri.27059.
Lee, L.E., Vavasour, I.M., Dvorak, A., Liu, H., Abel, S., Johnson, P., Ristow, S., Au, S., Laule, C., Tam, R., Li, D.K.B.K., Cross, H., Ackermans, N., Schabas, A.J., Chan, J., Sayao, A.-L.-L., Devonshire, V., Carruthers, R., Traboulsee, A., Kolind, S., 2021. Cervical cord myelin abnormality is associated with clinical disability in multiple sclerosis. Mult. Scler. J. 27, 2191–2198. https://doi.org/10.1177/13524585211001780.
Lefeuvre, J., Duan, Q., de Zwart, J., van Gelderen, P., Lehericy, S., Jacobson, S., Reich, D., Nair, G., 2016. MRI of the Thoracic Spinal Cord in Multiple Sclerosis at 7T. Proc. Annu. Meet. ISMRM.
Lema, A., Bishop, C., Malik, O., Mattoscio, M., Ali, R., Nicholas, R., Muraro, P.A., Matthews, P.M., Waldman, A.D., Newbould, R.D., 2016. A compararison of magnetization transfer methods to assess brain and cervical cord microstructure in multiple sclerosis. J. Neuroimaging 1–6. https://doi.org/10.1111/jon.12377.
Lévy, S., Guertin, M.C., Khatibi, A., Mezer, A., Martinu, K., Chen, J.I., Stikov, N., Rainville, P., Cohen-Adad, J., 2018. Test-retest reliability of myelin imaging in the human spinal cord: Measurement errors versus region- and aging-induced variations. PLoS One 13, e0189944. doi: 10.1371/journal.pone.0189944.
Lévy, S., Rapacchi, S., Massire, A., Troalen, T., Feiweier, T., Guye, M., Callot, V., 2020. Intravoxel Incoherent Motion at 7 Tesla to quantify human spinal cord perfusion: limitations and promises. Magn. Reson. Med. 84, 1198–1217. https://doi.org/10.1002/MRM.28195.
Liu, H., Ljungberg, E., Dvorak, A.V., Lee, L.E., Yik, J.T., MacMillan, E.L., Barlow, L., Li, D.K.B., Traboulsee, A., Kolind, S.H., Kramer, J.L.K., Laule, C., 2020a. Myelin water fraction and intra/extracellular water geometric mean T2 normative atlases for the cervical spinal cord from 3T MRI. J. Neuroimaging 30, 50–57. https://doi.org/10.1111/JON.12659.
Liu, Y., Lukas, C., Steenwijk, M.D., Daams, M., Versteeg, A., Duan, Y., Li, K., Weiler, F., Hahn, H.K., Wattjes, M.P., Barkhof, F., Vrenken, H., 2016. Multicenter Validation of Mean Upper Cervical Cord Area Measurements from Head 3D T1-Weighted MR Imaging in Patients with Multiple Sclerosis 37, 749–754.
Liu, H., Xiang, Q.-S., Tam, R., Dvorak, A.V., MacKay, A.L., Kolind, S.H., Traboulsee, A., Vavasour, I.M., Li, D.K.B., Kramer, J.K., Laule, C., 2020b. Myelin water imaging data analysis in less than one minute. Neuroimage 210, 116551. https://doi.org/10.1016/j.neuroimage.2020.116551.
Liu, Z., Yaldizli, Ö., Pardini, M., Sethi, V., Kearney, H., Muhlert, N., Wheeler-Kingshott, C., Miller, D.H., Chard, D.T., 2015. Cervical cord area measurement using volumetric brain magnetic resonance imaging in multiple sclerosis. Mult. Scler. Relat. Disord. 4, 52–57. https://doi.org/10.1016/J.MSARD.2014.11.004.
Ljungberg, E., Vavasour, I., Tam, R., Yoo, Y., Rauscher, A., Li, D.K.B., Traboulsee, A., MacKay, A., Kolind, S., 2017. Rapid myelin water imaging in human cervical spinal cord. Magn. Reson. Med. 78, 1482–1487. https://doi.org/10.1002/mrm.26551.
Lukas, C., Bellenberg, B., Prados, F., Valsasina, P., Parmar, K., Brouwer, I., Pareto, D., Rovira, À., Sastre-Garriga, J., Gandini Wheeler-Kingshott, C.A.M., Kappos, L., Rocca, M.A., Filippi, M., Yiannakas, M., Barkhof, F., Vrenken, H., 2021. Quantification of cervical cord cross-sectional area: which acquisition, vertebra level, and analysis software? A multicenter repeatability study on a traveling healthy volunteer. Front. Neurol. 12, 16.
Lundell, H., Nilsson, M., Dyrby, T.B., Parker, G.J.M., Cristinacce, P.L.H., Zhou, F.L., Topgaard, D., Lasič, S., 2019. Multidimensional diffusion MRI with spectrally modulated gradients reveals unprecedented microstructural detail. Sci. Rep. 9 https://doi.org/10.1038/s41598-019-45235-7.
MacKay, A.L., Laule, C., 2016. Magnetic resonance of myelin water: an in vivo marker for myelin. Brain Plast. 2, 71–91. https://doi.org/10.3233/BPL-160033.
Massire, A., Demortière, S., Lehmann, P., Rasoanandrianina, H., Guye, M., Audoin, B., Pelletier, J., Callot, V., 2019. High-resolution multiparametric quantitative MRI of the cervical spinal cord at 7T: preliminary results at the early stage of multiple sclerosis. Proc. Annu. Meet. ISMRM.
Massire, A., Ph, D., Feiweier, T., Ph, D., Kober, T., Ph, D., Troalen, T., Ph, D., Ranjeva, J., Ph, D., Guye, M., Ph, D., Callot, V., Ph, D., 2018a. MR imaging of the cervical spinal cord at 7T : a multiparametric portfolio 2–9.
Massire, A., Rasoanandrianina, H., Taso, M., Guye, M., Ranjeva, J.P., Feiweier, T., Callot, V., 2018. Feasibility of single-shot multi-level multi-angle diffusion tensor imaging of the human cervical spinal cord at 7T. Magn. Reson. Med. 80, 947–957. https://doi.org/10.1002/MRM.27087.
Massire, A., Rasoanandrianina, H., Guye, M., Callot, V., 2020. Anterior fissure, central canal, posterior septum and more: New insights into the cervical spinal cord gray and white matter regional organization using T1 mapping at 7T. Neuroimage 205, 116275. https://doi.org/10.1016/j.neuroimage.2019.116275.
McDowell, A.R., Petrova, N., Carassiti, D., Miquel, M.E., Thomas, D.L., Barker, G.J., Schmierer, K., Wood, T.C., 2022. High-resolution quantitative MRI of multiple sclerosis spinal cord lesions. Magn. Reson. Med. 87, 2914–2921. https://doi.org/10.1002/MRM.29152.
Mina, Y., Azodi, S., Dubuche, T., Andrada, F., Osuorah, I., Ohayon, J., Cortese, I., Wu, T., Johnson, K.R., Reich, D.S., Nair, G., Jacobson, S., 2021. Cervical and thoracic cord atrophy in multiple sclerosis phenotypes: quantification and correlation with clinical disability. NeuroImage Clin. 30, 102680 https://doi.org/10.1016/J.NICL.2021.102680.
Mirafzal, S., Goujon, A., Deschamps, R., Zuber, K., Sadik, J.C., Gout, O., Lecler, A., Savatovsky, J., 2020. 3D PSIR MRI at 3 Tesla improves detection of spinal cord lesions in multiple sclerosis. J. Neurol. 267, 406–414. https://doi.org/10.1007/s00415-019-09591-8.
Moccia, M., Ciccarelli, O., 2017. Molecular and metabolic imaging in multiple sclerosis. Neuroimaging Clin. N. Am. 27, 343–356. https://doi.org/10.1016/J.NIC.2016.12.005.
Moccia, M., Ruggieri, S., Ianniello, A., Toosy, A., Pozzilli, C., Ciccarelli, O., 2019. Advances in spinal cord imaging in multiple sclerosis. Ther. Adv. Neurol. Disord. 12, 175628641984059. doi: 10.1177/1756286419840593.
Moccia, M., Valsecchi, N., Ciccarelli, O., Van Schijndel, R., Barkhof, F., Prados, F., 2020. Spinal cord atrophy in a primary progressive multiple sclerosis trial: improved sample size using GBSI. NeuroImage Clin. 28, 102418 https://doi.org/10.1016/j.nicl.2020.102418.
Msayib, Y., Harston, G.W.J., Tee, Y.K., Sheerin, F., Blockley, N.P., Okell, T.W., Jezzard, P., Kennedy, J., Chappell, M.A., 2019. Quantitative CEST imaging of amide proton transfer in acute ischaemic stroke. NeuroImage Clin. 23, 101833.
Mühlau, M., 2022. T1/T2-weighted ratio is a surrogate marker of demyelination in multiple sclerosis: No. Mult. Scler. J. 28, 355–356. https://doi.org/10.1177/13524585211063622.
Nakamura, K., Zheng, Y., Ontaneda, D., 2022. T1/T2-weighted ratio is a surrogate marker of demyelination in multiple sclerosis—yes. Mult. Scler. J. 28, 352–354. https://doi.org/10.1177/13524585211066313.
Nery, F., Szczepankiewicz, F., Kerkelä, L., Hall, M.G., Kaden, E., Gordon, I., Thomas, D.L., Clark, C.A., 2019. In vivo demonstration of microscopic anisotropy in the human kidney using multidimensional diffusion MRI. Magn. Reson. Med. 82, 2160–2168. https://doi.org/10.1002/MRM.27869.
Novikov, D.S., Kiselev, V.G., Jespersen, S.N., 2018. On modeling. Magn. Reson. Med. 79, 3172–3193. https://doi.org/10.1002/MRM.27101.
Novikov, D.S., Fieremans, E., Jespersen, S.N., Kiselev, V.G., 2019. Quantifying brain microstructure with diffusion MRI: theory and parameter estimation. NMR Biomed. 32, e3998.
Oudejans, E., Luchicchi, A., Strijbis, E.M.M., Geurts, J.J.G., van Dam, A.-M., 2021. Is MS affecting the CNS only? Neurol. – Neuroimmunol. Neuroinflammation 8 (1), e914.
Ouellette, R., Mangeat, G., Polyak, I., Warntjes, M., Forslin, Y., Bergendal, Å., Plattén, M., Uppman, M., Treaba, C.A., Cohen-Adad, J., Piehl, F., Kristoffersen Wiberg, M., Fredrikson, S., Mainero, C., Granberg, T., Cohen-Adad, J., Piehl, F., Kristoffersen

Wiberg, M., Fredrikson, S., Mainero, C., Granberg, T., 2020a. Validation of rapid magnetic resonance myelin imaging in multiple sclerosis. Ann. Neurol. 87, 710–724. https://doi.org/10.1002/ana.25705.

Ouellette, R., Treaba, C.A., Granberg, T., Herranz, E., Barletta, V., Mehndiratta, A., De Leener, B., Tauhid, S., Yousuf, F., Dupont, S.M., Klawiter, E.C., Sloane, J.A., Bakshi, R., Cohen-Adad, J., Mainero, C., 2020b. 7 T imaging reveals a gradient in spinal cord lesion distribution in multiple sclerosis. Brain 143, 2973–2987. https://doi.org/10.1093/brain/awaa249.

Palombo, M., Ianus, A., Guerreri, M., Nunes, D., Alexander, D.C., Shemesh, N., Zhang, H., 2020. SANDI: a compartment-based model for non-invasive apparent soma and neurite imaging by diffusion MRI. Neuroimage 215, 116835.

Papinutto, N., Bakshi, R., Bischof, A., Calabresi, P.A., Caverzasi, E., Constable, R.T., Datta, E., Kirkish, G., Nair, G., Oh, J., Pelletier, D., Pham, D.L., Reich, D.S., Rooney, W., Roy, S., Schwartz, D., Shinohara, R.T., Sicotte, N.L., Stern, W.A., Tagge, I., Tauhid, S., Tummala, S., Henry, R.G., 2018. Gradient nonlinearity effects on upper cervical spinal cord area measurement from 3D T1-weighted brain MRI acquisitions. Magn. Reson. Med. 79 (3), 1595–1601.

Papinutto, N., Henry, R.G., 2019. Evaluation of intra- and interscanner reliability of MRI protocols for spinal cord gray matter and total cross-sectional area measurements. J. Magn. Reson. Imaging 49, 1078–1090. https://doi.org/10.1002/jmri.26269.

Papinutto, N., Schlaeger, R., Panara, V., Zhu, A.H., Caverzasi, E., Stern, W.A., Hauser, S. L., Henry, R.G., Fehlings, M., 2015. Age, gender and normalization covariates for spinal cord gray matter and total cross-sectional areas at cervical and thoracic levels: a 2D phase sensitive inversion recovery imaging study. PLoS One 10 (3), e0118576.

Pasternak, O., Sochen, N., Gur, Y., Intrator, N., Assaf, Y., 2009. Free water elimination and mapping from diffusion MRI. Magn. Reson. Med. 62, 717–730. https://doi.org/10.1002/MRM.22055.

Perone, C.S., Calabrese, E., Cohen-Adad, J., 2018. Spinal cord gray matter segmentation using deep dilated convolutions. Sci. Rep. 8 (1).

Prados, F., Ashburner, J., Blaiotta, C., Brosch, T., Carballido-Gamio, J., Cardoso, M.J., Conrad, B.N., Datta, E., Dávid, G., Leener, B.D., Dupont, S.M., Freund, P., Wheeler-Kingshott, C.A.M.G., Grussu, F., Henry, R., Landman, B.A., Ljungberg, E., Lyttle, B., Ourselin, S., Papinutto, N., Saporito, S., Schlaeger, R., Smith, S.A., Summers, P., Tam, R., Yiannakas, M.C., Zhu, A., Cohen-Adad, J., 2017. Spinal cord grey matter segmentation challenge. Neuroimage 152, 312–329. https://doi.org/10.1016/j.neuroimage.2017.03.010.

Qiao, Y., Shi, Y., 2020. Unsupervised deep learning for susceptibility distortion correction in connectome imaging. Med. Image Comput. Comput. Assist. Interv. 12267, 302–310. https://doi.org/10.1007/978-3-030-59728-3_30.

Rasoanandrianina, H., Demortière, S., Trabelsi, A., Ranjeva, J.P., Girard, O., Duhamel, G., Guye, M., Pelletier, J., Audoin, B., Callot, V., 2020. Sensitivity of the inhomogeneous magnetization transfer imaging technique to spinal cord damage in multiple sclerosis. Am. J. Neuroradiol. 41, 929–937. https://doi.org/10.3174/AJNR.A6554.

Rocca, M.A., Absinta, M., Valsasina, P., Copetti, M., Caputo, D., Comi, G., Filippi, M., 2012. Abnormal cervical cord function contributes to fatigue in multiple sclerosis. Mult. Scler. J. 18, 1552–1559. https://doi.org/10.1177/1352458512440516.

Rovaris, M., Bozzali, M., Santuccio, G., Iannucci, G., Sormani, M.P., Colombo, B., Comi, G., Filippi, M., 2000. Relative contributions of brain and cervical cord pathology to multiple sclerosis disability: a study with magnetisation transfer ratio histogram analysis. J. Neurol. Neurosurg. Psychiatry 69, 723–727. https://doi.org/10.1136/JNNP.69.6.723.

Rovaris, M., Bozzali, M., Santuccio, G., Ghezzi, A., Caputo, D., Montanari, E., Bertolotto, A., Bergamaschi, R., Capra, R., Mancardi, G., Martinelli, V., Comi, G., Filippi, M., 2001. In vivo assessment of the brain and cervical cord pathology of patients with primary progressive multiple sclerosis. Brain 124, 2540–2549. https://doi.org/10.1093/BRAIN/124.12.2540.

Rovaris, M., Judica, E., Sastre-Garriga, J., Rovira, A., Sormani, M.P., Benedetti, B., Korteweg, T., De Stefano, N., Khaleeli, Z., Montalban, X., Barkhof, F., Miller, D.H., Polman, C., Thompson, A.J., Filippi, M., 2008. Large-scale, multicentre, quantitative MRI study of brain and cord damage in primary progressive multiple sclerosis. Mult. Scler. 14, 455–464. https://doi.org/10.1177/1352458507085129.

Ruggieri, S., Petracca, M., Miller, A., Krieger, S., Ghassemi, R., Bencosme, Y., Riley, C., Howard, J., Lublin, F., Inglese, M., 2015. Association of deep gray matter damage with cortical and spinal cord degeneration in primary progressive multiple sclerosis. JAMA Neurol. 72, 1466–1474. https://doi.org/10.1001/JAMANEUROL.2015.1897.

Ruggieri, S., Petracca, M., De Giglio, L., De Luca, F., Giannì, C., Gurreri, F., Petsas, N., Tommasin, S., Pozzilli, C., Pantano, P., 2021. A matter of atrophy: differential impact of brain and spine damage on disability worsening in multiple sclerosis. J. Neurol. 268, 4698–4706. https://doi.org/10.1007/s00415-021-10576-9.

Samaraweera, A.P.R., Clarke, M.A., Whitehead, A., Falah, Y., Driver, I.D., Dineen, R.A., Morgan, P.S., Evangelou, N., 2017. The central vein sign in multiple sclerosis lesions is present irrespective of the T2* sequence at 3 T. J. Neuroimaging 27, 114–121. https://doi.org/10.1111/JON.12367.

Sastre-Garriga, J., Pareto, D., Alberich, M., Rodríguez-Acevedo, B., Vidal-Jordana, À., Corral, J.F., Tintoré, M., Río, J., Auger, C., Montalban, X., Rovira, À., 2022a. Spinal cord grey matter atrophy in Multiple Sclerosis clinical practice. Neurosci. Informatics 2 (2), 100071.

Sastre-Garriga, J., Rovira, A., García-Vidal, A., Carbonell-Mirabent, P., Alberich, M., Auger, C., Tintoré, M., Montalban, X., Pareto, D., 2022b. Defining the spinal cord reserve concept in multiple sclerosis – measurement and association with disability of the spinal cord canal area (S26.006). Neurology 98, 2551.

Sati, P., Oh, J., Constable, R.T., Evangelou, N., Guttmann, C.R.G., Henry, R.G., Klawiter, E.C., Mainero, C., Massacesi, L., McFarland, H., Nelson, F., Ontaneda, D., Rauscher, A., Rooney, W.D., Samaraweera, A.P.R., Shinohara, R.T., Sobel, R.A., Solomon, A.J., Treaba, C.A., Wuerfel, J., Zivadinov, R., Sicotte, N.L., Pelletier, D., Reich, D.S., 2016. The central vein sign and its clinical evaluation for the diagnosis of multiple sclerosis: a consensus statement from the North American Imaging in Multiple Sclerosis Cooperative. Nat. Rev. Neurol. 12 (12), 714–722.

Schilling, K.G., Blaber, J., Huo, Y., Newton, A., Hansen, C., Nath, V., Shafer, A.T., Williams, O., Resnick, S.M., Rogers, B., Anderson, A.W., Landman, B.A., 2019a. Synthesized b0 for diffusion distortion correction (Synb0-DisCo). Magn. Reson. Imaging 64, 62–70. https://doi.org/10.1016/J.MRI.2019.05.008.

Schilling, K.G., By, S., Feiler, H.R., Box, B.A., O'Grady, K.P., Witt, A., Landman, B.A., Smith, S.A., 2019b. Diffusion MRI microstructural models in the cervical spinal cord – application, normative values, and correlations with histological analysis. Neuroimage 201, 116026.

Schilling, K.G., Blaber, J., Hansen, C., Cai, L., Rogers, B., Anderson, A.W., Smith, S., Kanakaraj, P., Rex, T., Resnick, S.M., Shafer, A.T., Cutting, L.E., Woodward, N., Zald, D., Landman, B.A., 2020. Distortion correction of diffusion weighted MRI without reverse phase-encoding scans or field-maps. PLoS One 15, e0236418.

Schilling, K.G., Fadnavis, S., Batson, J., Visagie, M., Combes, A.J.E., McKnight, C.D., Bagnato, F., Garyfallidis, E., Landman, B.A., Smith, S.A., O'Grady, K.P., 2021. Patch2Self denoising of diffusion MRI in the cervical spinal cord improves intra-cord contrast, signal modelling, repeatability, and feature conspicuity. medRxiv 2021.10.04.21264389. doi: 10.1101/2021.10.04.21264389.

Schlaeger, R., Papinutto, N., Panara, V., Bevan, C., Lobach, I.V., Bucci, M., Caverzasi, E., Gelfand, J.M., Green, A.J., Jordan, K.M., Stern, W.A., Von Büdingen, H.C., Waubant, E., Zhu, A.H., Goodin, D.S., Cree, B.A.C., Hauser, S.L., Henry, R.G., 2014. Spinal cord gray matter atrophy correlates with multiple sclerosis disability. Ann. Neurol. 76, 568–580. https://doi.org/10.1002/ana.24241.

Schlaeger, R., Papinutto, N., Zhu, A.H., Lobach, I.V., Bevan, C.J., Bucci, M., Castellano, A., Gelfand, J.M., Graves, J.S., Green, A.J., Jordan, K.M., Keshavan, A., Panara, V., Stern, W.A., Von Büdingen, H.C., Waubant, E., Goodin, D.S., Cree, B.A.C., Hauser, S.L., Henry, R.G., 2015. Association between thoracic spinal cord gray matter atrophy and disability in multiple sclerosis. JAMA Neurol. 72, 897–904. https://doi.org/10.1001/JAMANEUROL.2015.0993.

Schmierer, K., Tozer, D.J., Scaravilli, F., Altmann, D.R., Barker, G.J., Tofts, P.S., Miller, D.H., 2007. Quantitative magnetization transfer imaging in postmortem multiple sclerosis brain. J. Magn. Reson. Imaging 26, 41–51. https://doi.org/10.1002/jmri.20984.

Schmierer, K., McDowell, A., Petrova, N., Carassiti, D., Thomas, D.L.L., Miquel, M.E.E., 2018. Quantifying multiple sclerosis pathology in post mortem spinal cord using MRI. Neuroimage 182, 251–258. https://doi.org/10.1016/j.neuroimage.2018.01.052.

Sinnecker, T., Clarke, M.A., Meier, D., Enzinger, C., Calabrese, M., De Stefano, N., Pitiot, A., Giorgio, A., Schoonheim, M.M., Paul, F., Pawlak, M.A., Schmidt, R., Kappos, L., Montalban, X., Rovira, À., Evangelou, N., Wuerfel, J., 2019. Evaluation of the Central Vein Sign as a Diagnostic Imaging Biomarker in Multiple Sclerosis. JAMA Neurol. 76, 1446–1456. https://doi.org/10.1001/JAMANEUROL.2019.2478.

Smith, A.K., Dortch, R.D., Dethrage, L.M., Smith, S.A., 2014. Rapid, high-resolution quantitative magnetization transfer MRI of the human spinal cord. Neuroimage 95, 106–116. https://doi.org/10.1016/j.neuroimage.2014.03.005.

Smith, A.K., By, S., Lyttle, B.D., Dortch, R.D., Box, B.A., Mckeithan, L.J., Thukral, S., Bagnato, F., Pawate, S., Smith, S.A., 2017. Evaluating single-point quantitative magnetization transfer in the cervical spinal cord: application to multiple sclerosis. NeuroImage. Clin. 16, 58–65. https://doi.org/10.1016/J.NICL.2017.07.010.

Snoussi, H., Cohen-Adad, J., Commowick, O., Combès, B., Bannier, É., Kerbrat, A., Barillot, C., Caruyer, E., Emmanuel Caruyer, C., Rennes, U., 2021. Evaluation of distortion correction methods in diffusion MRI of the spinal cord. doi: 10.48550/arxiv.2108.03817.

Solanky, B.S., Riemer, F., Golay, X., Wheeler-Kingshott, C.A.M., 2013. Sodium quantification in the spinal cord at 3T. Magn. Reson. Med. 69, 1201–1208. https://doi.org/10.1002/MRM.24696.

Solanky, B.S., Prados, F., Tur, C., Yiannakas, M.C., Kanber, B., Cawley, N., Brownlee, W., Ourselin, S., Golay, X., Ciccarelli, O., Gandini Wheeler-Kingshott, C.A.M., 2020. Sodium in the relapsing-remitting multiple sclerosis spinal cord: increased concentrations and associations with microstructural tissue anisotropy. J. Magn. Reson. Imaging 52, 1429–1438. https://doi.org/10.1002/JMRI.27201.

Song, X., Li, D., Qiu, Z., Su, S., Wu, Y., Wang, J., Liu, Z., Dong, H., 2020. Correlation between EDSS scores and cervical spinal cord atrophy at 3T MRI in multiple sclerosis: a systematic review and meta-analysis. Mult. Scler. Relat. Disord. 37, 101426 https://doi.org/10.1016/J.MSARD.2019.101426.

Sun, P.Z., Zhou, J., Huang, J., Van Zijl, P., 2007. Simplified quantitative description of amide proton transfer (APT) imaging during acute ischemia. Magn. Reson. Med. 57, 405–410. https://doi.org/10.1002/MRM.21151.

Swanberg, K.M., Landheer, K., Pitt, D., Juchem, C., 2019. Quantifying the metabolic signature of multiple sclerosis by in vivo proton magnetic resonance spectroscopy: current challenges and future outlook in the translation from proton signal to diagnostic biomarker. Front. Neurol. 10 https://doi.org/10.3389/FNEUR.2019.01173.

Taheri, K., Vavasour, I.M., Abel, S., Lee, L.E., Johnson, P., Ristow, S., Tam, R., Laule, C., Ackermans, N.C., Schabas, A., Cross, H., Chan, J.K., Sayao, A.-L., Bhan, V., Devonshire, V., Carruthers, R., Li, D.K.B., Traboulsee, A.L., Kolind, S.H., Dvorak, A. V., 2022. Cervical spinal cord atrophy can be accurately quantified using head images. Mult. Scler. J. - Exp. Transl. Clin. 8, 205521732110707. doi: 10.1177/20552173211070760.

Taso, M., Le Troter, A., Sdika, M., Cohen-Adad, J., Arnoux, P.J., Guye, M., Ranjeva, J.P., Callot, V., 2015. A reliable spatially normalized template of the human spinal cord – applications to automated white matter/gray matter segmentation and tensor-based morphometry (TBM) mapping of gray matter alterations occurring with age. Neuroimage 117, 20–28. https://doi.org/10.1016/j.neuroimage.2015.05.034.

Tax, C.M.W., Otte, W.M., Viergever, M.A., Dijkhuizen, R.M., Leemans, A., 2015. REKINDLE: Robust Extraction of Kurtosis INDices with linear estimation. Magn. Reson. Med. 73, 794–808. https://doi.org/10.1002/MRM.25165/ASSET/SUPINFO/MRM25165-SUP-0006-SUPPFIG6.TIF.

Tax, C.M.W., Bastiani, M., Veraart, J., Garyfallidis, E., Okan Irfanoglu, M., 2022. What's new and what's next in diffusion MRI preprocessing. Neuroimage 249, 118830.

Teraguchi, M., Yamada, H., Yoshida, M., Nakayama, Y., Kondo, T., Ito, H., Terada, M., Kaneoke, Y., 2014. Contrast enrichment of spinal cord MR imaging using a ratio of T1-weighted and T2-weighted signals. J. Magn. Reson. Imaging 40, 1199–1207. https://doi.org/10.1002/JMRI.24456.

Tinnermann, A., Büchel, C., Cohen-Adad, J., 2021. Cortico-spinal imaging to study pain. Neuroimage 224, 117439. https://doi.org/10.1016/j.neuroimage.2020.117439.

Toosy, A.T., Kou, N., Altmann, D., Wheeler-Kingshott, C.A.M., Thompson, A.J., Ciccarelli, O., 2014. Voxel-based cervical spinal cord mapping of diffusion abnormalities in MS-related myelitis. Neurology 83, 1321–1325. https://doi.org/10.1212/WNL.0000000000000857.

Topgaard, D., 2017. Multidimensional diffusion MRI. J. Magn. Reson. 275, 98–113. https://doi.org/10.1016/J.JMR.2016.12.007.

Toufani, H., Vard, A., Adibi, I., 2021. A pipeline to quantify spinal cord atrophy with deep learning: application to differentiation of MS and NMOSD patients. Phys. Medica 89, 51–62. https://doi.org/10.1016/J.EJMP.2021.07.030.

Traboulsee, A., Simon, J.H., Stone, L., Fisher, E., Jones, D.E., Malhotra, A., Newsome, S. D., Oh, J., Reich, D.S., Richert, N., Rammohan, K., Khan, O., Radue, E.-W., Ford, C., Halper, J., Li, D., 2016. Revised recommendations of the consortium of MS centers task force for a standardized MRI protocol and clinical guidelines for the diagnosis and follow-up of multiple sclerosis. AJNR Am. J. Neuroradiol. 37 (3), 394–401.

Vahdat, S., Khatibi, A., Lungu, O., Finsterbusch, J., Büchel, C., Cohen-Adad, J., Marchand-Pauvert, V., Doyon, J., 2020. Resting-state brain and spinal cord networks in humans are functionally integrated. PLOS Biol. 18, e3000789. doi: 10.1371/journal.pbio.3000789.

Vaithianathar, L., Tench, C.R., Morgan, P.S., Constantinescu, C.S., 2003. Magnetic resonance imaging of the cervical spinal cord in multiple sclerosis: a quantitative T1 relaxation time mapping approach. J. Neurol. 250, 307–315. https://doi.org/10.1007/s00415-003-1001-8.

Valsasina, P., Agosta, F., Absinta, M., Sala, S., Caputo, D., Filippi, M., 2010. Cervical cord functional MRI changes in relapse-onset MS patients. J. Neurol. Neurosurg. Psychiatry 81, 405–408. https://doi.org/10.1136/jnnp.2009.187526.

Valsasina, P., Rocca, M.A., Absinta, M., Agosta, F., Caputo, D., Comi, G., Filippi, M., 2012. Cervical cord FMRI abnormalities differ between the progressive forms of multiple sclerosis. Hum. Brain Mapp. 33, 2072–2080. https://doi.org/10.1002/hbm.21346.

Valsasina, P., Rocca, M.A., Horsfield, M.A., Absinta, M., Messina, R., Caputo, D., Comi, G., Filippi, M., 2013. Regional cervical cord atrophy and disability in multiple sclerosis: a voxel-based analysis. Radiology 266, 853–861. https://doi.org/10.1148/RADIOL.12120813.

van der Weijden, C.W.J., García, D.V., Borra, R.J.H., Thurner, P., Meilof, J.F., van Laar, P.-J.-J., Dierckx, R.A.J.O., Gutmann, I.W., de Vries, E.F.J., 2021. Myelin quantification with MRI: a systematic review of accuracy and reproducibility. Neuroimage 226, 117561. https://doi.org/10.1016/j.neuroimage.2020.117561.

Van Obberghen, E., Mchinda, S., Le Troter, A., Prevost, V.H., Viout, P., Guye, M., Varma, G., Alsop, D.C., Ranjeva, J.P., Pelletier, J., Girard, O., Duhamel, G., 2018. Evaluation of the sensitivity of inhomogeneous magnetization transfer (ihMT) MRI for multiple sclerosis. AJNR Am. J. Neuroradiol. 39, 634–641. https://doi.org/10.3174/AJNR.A5563.

Van Zijl, P.C.M., Yadav, N.N., 2011. Chemical exchange saturation transfer (CEST): what is in a name and what isn't? Magn. Reson. Med. 65, 927–948. https://doi.org/10.1002/MRM.22761.

Vavasour, I.M., Laule, C., Li, D.K.B., Traboulsee, A.L., MacKay, A.L., 2011. Is the magnetization transfer ratio a marker for myelin in multiple sclerosis? J. Magn. Reson. Imaging 33, 710–718. https://doi.org/10.1002/jmri.22441.

Veraart, J., Novikov, D.S., Christiaens, D., Ades-aron, B., Sijbers, J., Fieremans, E., 2016. Denoising of diffusion MRI using random matrix theory. Neuroimage 142, 394–406. https://doi.org/10.1016/J.NEUROIMAGE.2016.08.016.

Veraart, J., Nunes, D., Rudrapatna, U., Fieremans, E., Jones, D.K., Novikov, D.S., Shemesh, N., 2020. Noninvasive quantification of axon radii using diffusion MRI. Elife 9. https://doi.org/10.7554/ELIFE.49855.

Warntjes, M., Engström, M., Tisell, A., Lundberg, P., 2016. Modeling the presence of myelin and edema in the brain based on multi-parametric quantitative MRI. Front. Neurol. 7 https://doi.org/10.3389/fneur.2016.00016.

Wattjes, M.P., Ciccarelli, O., Reich, D.S., Banwell, B., de Stefano, N., Enzinger, C., Fazekas, F., Filippi, M., Frederiksen, J., Gasperini, C., Hacohen, Y., Kappos, L., Li, D. K.B.B., Mankad, K., Montalban, X., Newsome, S.D., Oh, J., Palace, J., Rocca, M.A.M. A., Sastre-Garriga, J., Tintoré, M., Traboulsee, A., Vrenken, H., Yousry, T., Barkhof, F., Rovira, À., Rocca, M.A.M.A., Tintore, M., Rovira, A., de Stefano, N., Enzinger, C., Fazekas, F., Filippi, M., Frederiksen, J., Gasperini, C., Hacohen, Y., Kappos, L., Li, D.K.B.B., Mankad, K., Montalban, X., Newsome, S.D., Oh, J., Palace, J., Rocca, M.A.M.A., Sastre-Garriga, J., Tintoré, M., Traboulsee, A., Vrenken, H., Yousry, T., Barkhof, F., Rovira, À., Wattjes, M.P., Ciccarelli, O., de Stefano, N., Enzinger, C., Fazekas, F., Filippi, M., Frederiksen, J., Gasperini, C., Hacohen, Y., Kappos, L., Mankad, K., Montalban, X., Palace, J., Rocca, M.A.M.A., Sastre-Garriga, J., Tintore, M., Vrenken, H., Yousry, T., Barkhof, F., Rovira, A., Li, D. K.B.B., Traboulsee, A., Newsome, S.D., Banwell, B., Oh, J., Reich, D.S., Reich, D.S., Oh, J., 2021. 2021 MAGNIMS–CMSC–NAIMS consensus recommendations on the use of MRI in patients with multiple sclerosis. Lancet Neurol. 20, 653–670. https://doi.org/10.1016/S1474-4422(21)00095-8.

Weber, C.E., Krämer, J., Wittayer, M., Gregori, J., Randoll, S., Weiler, F., Heldmann, S., Roßmanith, C., Platten, M., Gass, A., Eisele, P., 2022. Association of iron rim lesions with brain and cervical cord volume in relapsing multiple sclerosis. Eur. Radiol. 32, 2012–2022. https://doi.org/10.1007/s00330-021-08233-w.

Weier, K., Mazraeh, J., Naegelin, Y., Thoeni, A., Hirsch, J.G., Fabbro, T., Bruni, N., Duyar, H., Bendfeldt, K., Radue, E.W., Kappos, L., Gass, A., 2012. Biplanar MRI for the assessment of the spinal cord in multiple sclerosis. Mult. Scler. J. 18, 1560–1569. https://doi.org/10.1177/1352458512442754.

Westin, C.F., Knutsson, H., Pasternak, O., Szczepankiewicz, F., Özarslan, E., van Westen, D., Mattisson, C., Bogren, M., O'Donnell, L.J., Kubicki, M., Topgaard, D., Nilsson, M., 2016. Q-space trajectory imaging for multidimensional diffusion MRI of the human brain. Neuroimage 135, 345–362. https://doi.org/10.1016/J.NEUROIMAGE.2016.02.039.

Wheeler-Kingshott, C.A.M., Cercignani, M., 2009. About "axial" and "radial" diffusivities. Magn. Reson. Med. 61, 1255–1260. https://doi.org/10.1002/mrm.21965.

Wilm, B.J., Svensson, J., Henning, A., Pruessmann, K.P., Boesiger, P., Kollias, S.S., 2007. Reduced field-of-view MRI using outer volume suppression for spinal cord diffusion imaging. Magn. Reson. Med. 57, 625–630. https://doi.org/10.1002/MRM.21167.

Witt, A., Reynolds, B., Conrad, B., Bhatia, A., Smith, S., 2019. 7T MRI Shows Enlarged Anterior Vein in the Spinal Cord of Multiple Sclerosis Patients. Proc. Annu. Meet. ISMRM.

Wu, T.-L., Yang, P.-F., Wang, F., Shi, Z., Mishra, A., Wu, R., Chen, L.M., Gore, J.C., 2019. Intrinsic functional architecture of the non-human primate spinal cord derived from fMRI and electrophysiology. Nat. Commun. 10, 1416. https://doi.org/10.1038/s41467-019-09485-3.

Yarnykh, V.L., 2012. Fast macromolecular proton fraction mapping from a single off-resonance magnetization transfer measurement. Magn. Reson. Med. 68, 166–178. https://doi.org/10.1002/MRM.23224.

Yoo, Y., Tang, L.Y.W., Li, D.K.B., Metz, L., Kolind, S., Traboulsee, A.L., Tam, R.C., 2019. Deep learning of brain lesion patterns and user-defined clinical and MRI features for predicting conversion to multiple sclerosis from clinically isolated syndrome. Comput. Methods Biomech. Biomed. Eng. Imaging Vis. 7, 250–259. https://doi.org/10.1080/21681163.2017.1356750.

York, E.N., Thrippleton, M.J., Meijboom, R., Hunt, D.P.J., Waldman, A.D., 2022. Quantitative magnetization transfer imaging in relapsing-remitting multiple sclerosis: a systematic review and meta-analysis. Brain Commun. 4 https://doi.org/10.1093/braincomms/fcac088.

Zhang, L., Chen, T., Tian, H., Xue, H., Ren, H., Li, L., Fan, Q., Wen, B., Ren, Z., 2019. Reproducibility of inhomogeneous magnetization transfer (ihMT): A test-retest, multi-site study. Magn. Reson. Imaging 57, 243–249. https://doi.org/10.1016/j.mri.2018.11.010.

Zhang, H., Schneider, T., Wheeler-Kingshott, C.A., Alexander, D.C., 2012. NODDI: practical in vivo neurite orientation dispersion and density imaging of the human brain. Neuroimage 61, 1000–1016. https://doi.org/10.1016/J.NEUROIMAGE.2012.03.072.